AD-A038 935 NATIONAL RESEARCH COUNCIL OF CANADA OTTAWA (ONTARIO) --ETC F/G 20/14
WAVE LOADS ON LARGE CIRCULAR CYLINDERS: A DESIGN METHOD (FORCES--ETC(U)
DEC 76 G R MOGRIDGE, W W JAMIESON

UNCLASSIFIED NL

1 OF 1
AD A038935

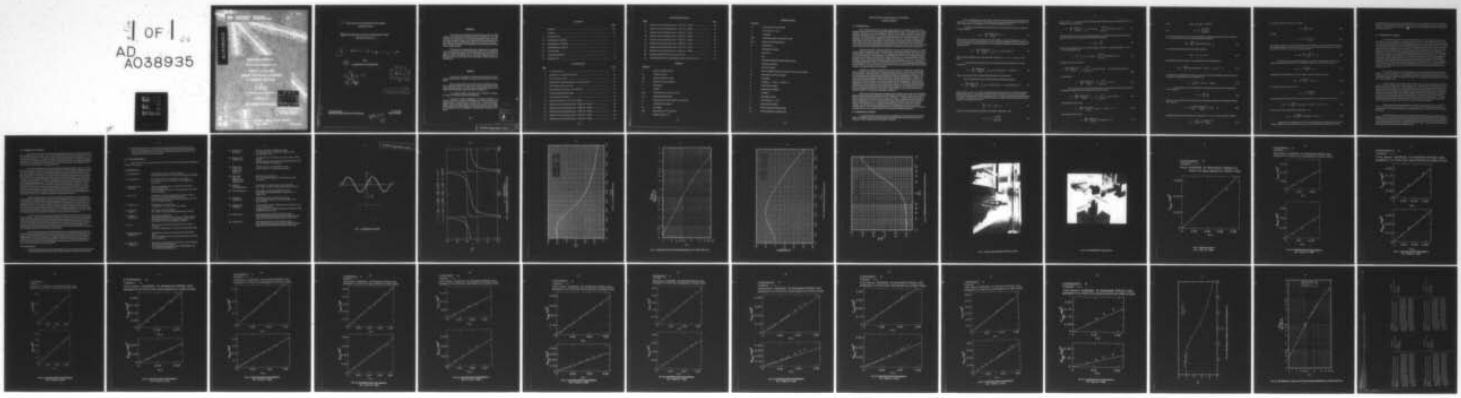

END

DATE FILMED
5-77

National Research Council Canada
Conseil national de recherches Canada

MH-111

B.S.

HYDRAULICS LABORATORY

MECHANICAL ENGINEERING REPORT

WAVE LOADS ON LARGE CIRCULAR CYLINDERS: A DESIGN METHOD

BY
G.R. MORRISON
W.M. JAMIESON

RAPPORT DE GÉNIE MÉCANIQUE

LABORATOIRE D'HYDRAULIQUE

OTTAWA, CANADA

NRC NO. 15827

(6) **WAVE LOADS ON LARGE CIRCULAR CYLINDERS: A DESIGN METHOD**

(FORCES DES HOULES SUR DES CYLINDRES CIRCULAIRES: METHODE DE CALCUL).

(9) Mechanical engineering rept.,

by/par

(10) **G.R. MOGRIDGE, W.W. JAMIESON**

(11) Dec 76

(12) 39 p.

J. Ploeg, Head/Chef
Hydraulics Laboratory/Laboratoire d'Hydraulique

D.C. MacPhail
Director/Directeur

SUMMARY

The forces and overturning moments exerted by waves on large vertical circular cylinders have been measured in the laboratory. Two rigid cylinders, 12 in. and 26.5 in. in diameter, extending from the bottom of a wave flume through the water surface, were tested in varying depths of water, for a range of wave periods and wave heights up to the point of breaking. A digital computer was used for the acquisition, processing, plotting and storage of the experimental data.

In addition to the experimental work, a design method is presented which allows the wave loads on large circular cylinders to be estimated by means of a simple desk calculation. The experimental data shows that this simple method of calculation, based on the linear diffraction theory of MacCamy and Fuchs, is accurate over a wide range of wave conditions and cylinder sizes.

RESUME

Les forces et les moments de renversement exercés par les houles sur des cylindres larges, circulaires et verticaux ont été mesurés dans le laboratoire.

Deux cylindres rigides de 12 et 26.5 pouces de diamètre, fixés au fond, s'étendant au-delà de la surface libre, ont été étudiés dans des différentes profondeurs d'eau. On a fait varier les périodes et les amplitudes des houles dans une large gamme jusqu'aux limites du déferlement.

Un ordinateur digital a été employé pour l'acquisition, l'analyse, le tracage et le stockage de données expérimentaux.

En plus de l'aspect expérimental, on présente également une méthode d'évaluation qui permet de déterminer les forces des houles sur des cylindres larges et circulaires, par un simple calcul. Les essais mettent en évidence que cette simple méthode de calcul qui est basée sur la théorie linèaire de diffraction de MacCamy et de Fuchs se prête à un large éventail des paramètres de houle et également à des différentes dimensions de cylindre.

CONTENTS

ILLUSTRATIONS

ILLUSTRATIONS (Cont'd)

SYMBOLS

Definition	
a	radius of a circular cylinder
C_m	coefficient of mass
C_m^*	modified coefficient of mass
D	diameter of a circular cylinder
d	water depth
e	2.71828 . . .
F(t)	horizontal force as a function of time
F_{max}	maximum horizontal force
f_x	horizontal force per unit length in the x direction
g	acceleration due to gravity
H	wave height
$H_m^{(1)}$	Hankel function of the first kind
i	complex operator $\sqrt{-1}$

SYMBOLS (Cont'd)

Definition	
J_m	Bessel function of the first kind
k	wave number, $k = 2\pi/L$
L	wavelength
$M(t)$	overturning moment as a function of time
M_{max}	maximum overturning moment
p	fluid pressure
r	radial polar co-ordinate
T	wave period
t	time
u	horizontal component of water particle velocity
x	horizontal co-ordinate
y	vertical co-ordinate
y_c	lever arm distance from point of action of F(t) to base of cylinder
Y_m	Bessel function of the second kind
α	phase angle
ϵ_m	constants, $\epsilon_0 = 1$ and $\epsilon_m = 2$ for $m \geqslant 1$
η	water surface elevation
θ	angular polar co-ordinate
π	3.141592 . . .
ρ	mass density of fluid
σ	wave frequency, $\sigma = 2\pi/T$
ϕ	total velocity potential
ϕ_I	velocity potential of incident waves
ϕ_R	velocity potential of reflected waves

WAVE LOADS ON LARGE CIRCULAR CYLINDERS: A DESIGN METHOD

1.0 INTRODUCTION

When considering wave forces on rigid circular cylinders, it is necessary to be aware of the differences between the wave forces on large and small diameter cylinders. If the diameter of a vertical cylinder is small relative to the wavelength, the wave force on the cylinder is normally calculated using the Morison equation (Morison et al.[13]) which consists of the sum of the inertial force and the viscous drag force. The Morison equation simplifies the general problem of wave structure interaction by assuming that the cylinder does not disturb the incident wave in any way. But as the diameter becomes large relative to the incident wavelength, the large diameter cylinder causes reflection and diffraction of the incident waves, the Morison equation does not apply and a diffraction theory must be used. Viscous drag forces are not important for wave heights which are small relative to the cylinder diameter, which is the usual case for large diameter cylinders and thus inertial forces are always predominant.

MacCamy and Fuchs[11] developed a diffraction theory for calculating wave loads on a vertical circular cylinder extending from above the water surface to the mudline; however, there are few experimental results to confirm their theory. Jen[8] has presented data agreeing with the theory but it is only for a very limited range of cylinder diameter on wavelength D/L up to 0.12. The experimental results of Lebreton and Cormault[10] are only for D/L equal to 0.09 and do not compare favourably with the diffraction theory. Data has been published by Watanabe and Horikawa[17] for D/L up to 0.4, but there are significant differences between the experimental results and the diffraction theory. Experiments by Chakrabarti and Tam[3] for D/L up to 0.54 and one test at D/L of 1.3, show agreement with MacCamy and Fuchs' theory; however, as with the other data there is very little information concerning the applicability of the theory for large wave steepnesses.

Chakrabarti[1] obtained an expression for the wave force on a cylinder due to Stokes' fifth-order wave theory, but the kinematic free surface boundary condition in the vicinity of the cylinder was not satisfied. Chakrabarti[2] later compared this approximate theory limited to the second order, to a second-order theory obtained using a perturbation method by Yamaguchi and Tsuchiya[18]. He found that although the experimental data obtained by Yamaguchi and Tsuchiya[18] correlated well with their second-order solution, his theory and experimental data showed that their solution overestimated the forces considerably. More recently, Raman and Venkatanarasaiah[15] have also used a perturbation method to develop a second-order diffraction theory. Unfortunately, the experimental results given to confirm the theory were obtained using a relatively small diameter cylinder for which previous authors have assumed that viscous drag forces are significant. The results would have been more convincing had the tests been conducted on a larger cylinder or had an attempt been made to separate the effects of viscosity and nonlinearity of the waves.

Wave loads on large floating and submerged bodies of different shapes have been determined using numerical techniques by Garrison and Chow[6], Hogben and Standing[7], Lebreton and Cormault[10], Garrett[5], Kokkinowrachos and Wilckens[9] and Van Oortmerssen[16]. Although these methods can be used to calculate the wave loads on circular cylinders, the computer programs are time consuming to develop and expensive to use. This report presents a design method based on the linear diffraction theory of MacCamy and Fuchs[11] to estimate wave forces and moments on large vertical circular cylinders. The method has been simplified so that only three graphs need be used to obtain the complete solution. Force and moment measurements on circular cylinders show that the theory gives a satisfactory solution over a large range of wave conditions and relative cylinder sizes.

2.0 THEORETICAL METHOD

Is is assumed that the fluid is inviscid and homogeneous and that the fluid motion is irrotational. The heights of the waves are small relative to the wavelengths so that terms involving wave steepness to second or higher order powers may be neglected.

The co-ordinates are chosen such that x is positive in the direction of wave propagation and y is positive in the upward direction. The origin of these co-ordinates is at still water level where the water surface elevation plotted against x has a maximum negative slope (Fig. 1).

According to small amplitude wave theory, the velocity potential of the waves incident on the rigid cylinder is

$$\phi_I = -\frac{gH}{2\sigma}\,\frac{\cos k(y+d)}{\cosh kd}\,e^{i(kx-\sigma t)} \tag{1}$$

where g is the acceleration due to gravity, H is the wave height, σ is the wave frequency, $\sigma = 2\pi/T$, T is the wave period, k is the wave number, $k = 2\pi/L$, L is the wavelength, d is the water depth, t is the time. The equation for plane incident waves can be expressed as an infinite series using the polar co-ordinates r and θ:

$$\phi_I = -\frac{gH}{2\sigma}\,\frac{\cosh k(y+d)}{\cosh kd}\,\sum_{m=0}^{\infty}\epsilon_m\, i^m\cos m\theta\, J_m(kr)\, e^{-i\sigma t} \tag{2}$$

where $J_m(kr)$ are Bessel functions of the first kind of orders 0, 1, 2 . . .m, $\epsilon_0 = 1$ and $\epsilon_m = 2$ for $m \geqslant 1$.

A cylindrical wave is reflected from the cylinder and may be described by the velocity potential ϕ_R:

$$\phi_R = -\frac{gH}{2\sigma}\,\frac{\cosh k(y+d)}{\cosh kd}\,\sum_{m=0}^{\infty}A_m\cos m\theta\,[J_m(kr) + i\,Y_m(kr)]\,e^{-i\sigma t} \tag{3}$$

where A_m are constants and $Y_m(kr)$ are Bessel functions of the second kind.

The total potential ϕ is the sum of the incident and reflected potentials:

$$\phi = -\frac{gH}{2\sigma}\,\frac{\cosh k(y+d)}{\cosh kd}\,\sum_{m=0}^{\infty}[\epsilon_m\, i^m\cos m\theta\, J_m(kr) + A_m\cos m\theta\, H_m^{(1)}(kr)]\,e^{-i\sigma t} \tag{4}$$

where $H_m^{(1)}(kr) = J_m(kr) + i\,Y_m(kr)$ is the Hankel function of the first kind. It should be noted that MacCamy and Fuchs[11] in their equation for the total potential, have incorrectly used the Hankel function of the second kind which in combination with $e^{-i\sigma t}$ defines a cylindrical wave moving towards the cylinder. The constants A_m are evaluated by using the boundary condition that the fluid velocity normal to the cylinder is zero, that is,

$$\frac{\partial\phi}{\partial r} = 0 \text{ at } r = D/2 = a \tag{5}$$

where D and a are the diameter and radius of the cylinder respectively. Thus,

$$A_m = -\epsilon_m\, i^m\,\frac{J'_m(ka)}{H'^{(1)}_m(ka)} \tag{6}$$

for m = 0, 1, 2, 3 . . ., where J'_m (ka) and $H'^{(1)}_m$ (ka) are the derivatives of J_m (kr) and $H^{(1)}_m$ (kr) at r = a. Therefore, the total potential is

$$\phi = -\frac{gH}{2\sigma} \frac{\cosh k(y+d)}{\cosh kd} \sum_{m=0}^{\infty} \epsilon_m i^m \left[J_m(kr) - \frac{J'_m(ka)}{H'^{(1)}_m(ka)} H^{(1)}_m(kr)\right] \cos m\theta \, e^{-i\sigma t} \tag{7}$$

The water surface elevation η and the dynamic pressure at the surface of the cylinder are calculated using the total velocity potential and the linear Bernoulli equation:

$$p = -\rho g y + \rho \frac{\partial \phi}{\partial t} \tag{8}$$

where p is the fluid pressure and ρ is the mass density of the fluid. At the water surface p = 0 and y = η, so from Equation (8),

$$\eta = \frac{H}{2} \sum_{m=0}^{\infty} \epsilon_m i^{m+1} \left[J_m(kr) - \frac{J'_m(ka)}{H'^{(1)}_m(ka)} H^{(1)}_m(kr)\right] \cos m\theta \, e^{-i\sigma t} \tag{9}$$

Similarly, the dynamic pressure is

$$p = \frac{\rho g H}{2} \frac{\cosh k(y+d)}{\cosh kd} \sum_{m=0}^{\infty} \frac{\epsilon_m i^{m+1}}{H'^{(1)}_m(ka)} \left[J_m(ka) H'^{(1)}_m(ka) - J'_m(ka) H^{(1)}_m(ka)\right] \cos m\theta \, e^{-i\sigma t} \tag{10}$$

which reduces to

$$p = -\frac{\rho g H}{\pi ka} \frac{\cosh k(y+d)}{\cosh kd} \sum_{m=0}^{\infty} \frac{\epsilon_m i^m}{H'^{(1)}_m(ka)} \cos m\theta \, e^{-i\sigma t} \tag{11}$$

The horizontal force in the longitudinal direction per unit length of cylinder is calculated by integrating the pressure given by Equation (11) around the cylinder:

$$f_x = \frac{2\rho g H}{\pi k} \frac{\cosh k(y+d)}{\cosh kd} \int_0^{\pi} \sum_{m=0}^{\infty} \frac{\epsilon_m i^m}{H'^{(1)}_m(ka)} \cos m\theta \cos\theta \, d\theta \, e^{-i\sigma t} \tag{12}$$

After integration this becomes

$$f_x = \frac{2\rho g H}{k} \frac{\cosh k(y+d)}{\cosh kd} \left[J'_1(ka) + i Y'_1(ka)\right]^{-1} i \, e^{-i\sigma t} \tag{13}$$

and taking the real part only,

$$f_x = \frac{2\rho g H}{k} \frac{\cosh k(y+d)}{\cosh kd} A(ka) \cos(\sigma t - \alpha) \tag{14}$$

where $$A(ka) = [J_1'^2(ka) + Y_1'^2(ka)]^{-1/2}$$

and $$\alpha = \tan^{-1}\left(\frac{J_1'(ka)}{Y_1'(ka)}\right)$$

The total horizontal force on the cylinder is obtained by integrating Equation (14) from the bottom $y = -d$, to the still water level $y = 0$, in keeping with linear theory:

$$F(t) = \frac{2\rho g H}{k^2} A(ka) \tanh kd \cos(\sigma t - \alpha) \tag{15}$$

The overturning moment about the base of the cylinder is

$$M(t) = \int_{-d}^{0} f_x (y + d)\, dy \tag{16}$$

Substituting for f_x from Equation (14) and carrying out the integration gives

$$M(t) = \frac{2\rho g H}{k^3} A(ka) [kd \tanh kd + \operatorname{sech} kd - 1] \cos(\sigma t - \alpha) \tag{17}$$

The distance y_c measured from the bottom to the point at which the resultant horizontal force acts is obtained by dividing Equation (17) by Equation (15):

$$y_c = \frac{L}{2\pi} [kd + \operatorname{csch} kd - \coth kd] \tag{18}$$

The horizontal force per unit length given by Equation (14) may be written equivalently as an inertia force:

$$f_x = C_m \frac{\rho \pi D^2}{4} \frac{du}{dt} \tag{19}$$

where C_m is the coefficient of mass and du/dt is the horizontal component of water particle acceleration. Therefore,

$$f_x = C_m \frac{\rho \pi^3 D^2 H}{2T^2} \frac{\cosh k(y + d)}{\sinh kd} \cos(kx - \sigma t) \tag{20}$$

Equating Equations (14) and (20) gives an expression for C_m at $x = 0$ at the centre of the cylinder:

$$C_m = \frac{4L^2}{\pi^3 D^2} A(ka) \frac{\cos(\sigma t - \alpha)}{\cos \sigma t} \tag{21}$$

A modified coefficient of mass C_m^* is defined as

$$C_m^* = \frac{4L^2}{\pi^3 D^2} A(ka) \tag{22}$$

such that

$$C_m = C_m^* \frac{\cos(\sigma t - \alpha)}{\cos \sigma t} \tag{23}$$

The coefficient of mass C_m is a function of time and varies through a wave cycle as shown in Figure 2. It is constant through the wave cycle only when α is zero, that is, for D/L approaching zero or approximately 0.59. When α is not zero, C_m is equal to C_m^* when

$$\sigma t = \tan^{-1}\left(\frac{1 - \cos\alpha}{\sin\alpha}\right) = \frac{\alpha}{2} \tag{24}$$

The total force in the longitudinal direction is obtained by integrating the force per unit length as given by Equation (20) for x = 0, through the depth of the water to still water level:

$$F(t) = C_m \frac{\rho\pi^2 D^2 HL}{4T^2} \cos \sigma t \tag{25}$$

Substituting the expression for C_m given by Equation (23) into Equation (25) gives

$$F(t) = C_m^* \frac{\rho\pi^2 D^2 HL}{4T^2} \cos(\sigma t - \alpha) \tag{26}$$

The maximum force occurs when $\sigma t = \alpha$:

$$F_{max} = C_m^* \frac{\rho\pi^2 D^2 HL}{4T^2} \tag{27}$$

The overturning moment about the base of the cylinder can also be expressed in terms of C_m^* as

$$M(t) = C_m^* \frac{\rho g HLD^2}{16} [kd \tanh kd + \operatorname{sech} kd - 1] \cos(\sigma t - \alpha) \tag{28}$$

The maximum overturning moment occurs when $\sigma t = \alpha$:

$$M_{max} = C_m^* \frac{\rho g HLD^2}{16} [kd \tanh kd + \operatorname{sech} kd - 1] \tag{29}$$

Figures 3, 4 and 5 are design curves based on the above equations. Figure 3 gives C_m^* by the solution of Equation (22), so that the force F_{max} may be calculated by using Equation (27). The

overturning moment about the base of the cylinder M_{max} given by Equation (29), can be obtained in Figure 4. The phase angle α is plotted in Figure 5 and allows the determination of F(t) and M(t) given by Equations (26) and (28) respectively. Moments may also be calculated by the product of the force and lever arm (Fig. 6).

3.0 EXPERIMENTAL METHOD

The circular cylinder (Fig. 7) used in the experiments was 12 in. in diameter and was constructed of 1/4 in. thick plexiglass. It was supported 1/8 in. above the wave flume bottom by a rigid 3 in. diameter steel tube clamped to a steel frame above the flume. A force meter was contained within the cylinder and consisted of two 3/4 in. diameter stainless steel strain rods 12 in. long. The wave force on the cylinder was transferred to the top strain rod through a horizontal steel bar and to the bottom strain rod through a circular steel base plate (Fig. 7). Foil strain gauges glued on the strain rods were aligned so that total horizontal forces could be measured in the direction of wave propagation and normal to the wave direction to give longitudinal and transverse forces respectively. The lower strain rod is visible in Figure 7, but the upper strain rod is hidden inside the 3 in. diameter tube. Also inside the tube are two solid bushings which fix one end of each of the strain rods. Using the Wheatstone bridge outputs from the upper and lower strain rods, it was possible to measure total forces and to calculate the corresponding overturning moments about the base of the cylinder. A more detailed description of the wave force meter and its calibration is given by Pratte et al.[14]. From the calibration curves of the force meter, its error band was estimated to be less than ±2% over the range of forces measured. The natural frequency of vibration of the cylinder in the maximum depth of water was approximately 11 Hz.

Wave profiles in the flume were measured by the noncontacting capacitive wave transducer (Zwarts[19,20]) shown in Figure 7. It was suspended above the water surface, midway between the cylinder and the flume wall where the wave heights measured were approximately equal to the incident wave heights measured without the cylinder in the flume. The wave flume was approximately 6 ft. wide, 4.5 ft. deep and 220 ft. long.

A limited number of tests were conducted using a 26.5 in. diameter cylinder to obtain force and moment data for larger values of relative diameter D/L. The cylinder was suspended from a force meter in a flume 12 ft. wide, 4.5 ft. deep and 162 ft. long. The force meter, shown in Figure 8 with a square-section cylinder attached to it, consisted of three aluminum strain members 3 in. in diameter. The strains in these members caused by wave loads were measured using semiconductor strain gauges forming six Wheatstone bridges. Three bridges measured strain due to bending and gave outputs proportional to the longitudinal, transverse and vertical forces. Three bridges measured strain due to torque and gave outputs proportional to the moments about the three co-ordinate axes. A detailed description of this force meter is given by Funke[4]. Wave heights were measured using a capacitive rod wave gauge at the location of the model but without the model in the flume.

Monochromatic waves were generated in five water depths ranging from 9.7 in. to 29.0 in. and seven wave periods were tested from 0.77 sec. to 2.58 sec. For each water depth and period, a number of waves were generated, ranging from small amplitude waves to those that were on the point of breaking.

A digital computer was used for the acquisition, processing, plotting and storage of data. Sampling of the data was commenced after the waves passing the model reached steady state conditions. For each test, the wave profile and the corresponding wave forces were sampled every one hundredth of a second for a total of six seconds. Total forces and overturning moments were computed and automatically plotted along with the wave profile measured at the cylinder. The experimental results were also printed and the data was stored on magnetic tape.

4.0 EXPERIMENTAL RESULTS

The number of waves in each test record varied depending on the wave period because of the fixed sampling time of six seconds. Any test with a variation in wave height or maximum force measurement within the record of more than 5% was not used. From the test records, the forces F_{max} and overturning moments M_{max} were taken as average absolute maximum values of positive and negative measurements. The difference between the positive values and the averages were normally less than 6%. The forces and corresponding moments measured in the transverse direction were negligible and are not included in the presentation of experimental results.

The maximum forces and moments were expressed nondimensionally as functions of wave steepness H/L, relative diameter D/L and relative depth d/L. This form of data presentation is used to show the variation of wave forces and moments with wave steepness. The graphs in Figures 9 to 22 show the comparison between the experimental results and the theoretical forces and moments calculated by Equations (27) and (29). In Figures 9 to 18 for which the relative diameter D/L is greater than 0.09, there is close agreement between the theory and experimental results. However, for D/L less than 0.09, the measured data differs considerably from the theory particularly for very small D/L and large wave steepness H/L. For this data, the absolute values of positive and negative wave loads are no longer approximately equal. They differ from their average values by as much as 8% for the data in Figure 20 for which D/L = 0.08 and 20% for the data in Figure 22 for which D/L = 0.057. In addition, for large wave steepnesses the phase angles between the wave load records and the wave profiles do not correspond to the theoretical values for α given in Equation (14). The phase angle increases with increasing wave steepness, which is typical of the effect of an increasing drag force. These characteristics of the experimental results are much more pronounced in the measurements of wave loads on square-section cylinders as described by Mogridge and Jamieson[1,2].

Although it appears that the deviations from theory described above are due primarily to viscous drag forces, similar deviations will occur due to nonlinearity of the waves. The lowest value of d/L measured was 0.09, for which experimental data is presented in Figure 16 and also Figure 22. In Figure 22, D/L is less than 0.09 indicating that there is a viscosity effect but the deviation of the experimental data from the theory could also be caused by the nonlinearity of the waves. The fact that it is not caused by nonlinearity is evident in Figure 16 where the experimental data agrees with the theory at the same value of relative depth d/L = 0.09. Mogridge and Jamieson[1,2] give test results for square-section cylinders in relative water depths to d/L = 0.06 and specify the limit of d/L = 0.09 at which nonlinearity of the waves causes deviation of results from the linear theory.

The test results were also plotted on the theoretical design curves developed from the linear diffraction theory. Using the measured absolute maximum forces with known values of wave height, length, period and cylinder size, C_m^* was calculated for varying values of D/L and plotted on the theoretical curve in Figure 23. Dimensionless moments were also calculated using the known values of C_m^* and were plotted on the theoretical curve in Figure 24. The data used is the average of a number of tests conducted with a range of wave steepnesses. For tests with D/L less than 0.09, the data averaged is from tests with wave steepnesses of less than 0.01. For D/L greater than 0.09, the data has been averaged for all tests run at each value of D/L and d/L.

The experimental data plotted in Figures 23 and 24 show good agreement with the linear diffraction theory for D/L between 0.057 and 0.441 and also for d/L between 0.090 and 0.786. The maximum wave steepness for which there is reasonable agreement between theory and experiment, depends mainly on the relative diameter D/L. Figures 9 to 22 indicate that above a value of D/L of 0.090, the theory may be used for wave steepnesses up to 0.076. However, for decreasing values of D/L, the theory can only be used for decreasing wave steepnesses, until at D/L equal to 0.057 the error at H/L equal to 0.018 is approximately 20%.

5.0 CONCLUSIONS

1. A simple design method based on the linear diffraction theory of MacCamy and Fuchs has been developed to determine the wave forces and overturning moments on large circular cylinders.

2. Results of experiments have shown that the theoretical method can be used over a wide range of conditions; that is, for D/L between 0.09 and 0.44, for d/L between 0.09 and 0.79 and for wave steepnesses up to 0.08. For D/L less than 0.09, the theory can be used with reasonable accuracy for low wave steepnesses.

6.0 ACKNOWLEDGEMENT

This project was part of a general study on wave forces initiated and funded by the Department of Public Works, Canada.

7.0 REFERENCES

1. Chakrabarti, S.K. — *Nonlinear Wave Forces on a Vertical Cylinder.* Proc. ASCE, Vol. 98, No. HY11, November 1972, pp. 1895-1909.

2. Chakrabarti, S.K. — *Second-Order Wave Force on Large Vertical Cylinder.* Proc. ASCE, Vol. 101, No. WW3, Tech. Note, August 1975, pp. 311-317.

3. Chakrabarti, S.K. Tam, W.A. — *Gross and Local Wave Loads on a Large Vertical Cylinder — Theory and Experiment.* Proc. Fifth Offshore Tech. Conf., Houston, Paper No. OTC 1818, 1973, pp. 813-826.

4. Funke, E.R. — *A Six Degree of Freedom Dynamometer for Measurement of Wave Forces on Models of Offshore Structures.* National Research Council Canada, DME, Hydraulics Lab. Tech. Rep. No. LTR-HY-54, 1976.

5. Garrett, C.J.R. — *Wave Forces on a Circular Dock.* J. Fluid Mech., Vol. 45, Pt. I, 1971, pp. 129-139.

6. Garrison, C.J. Chow, P.Y. — *Wave Forces on Submerged Bodies.* Proc. ASCE, Vol. 98, No. WW3, August 1972, pp. 375-392.

7. Hogben, N. Standing, R.G. — *Wave Loads on Large Bodies.* International Symposium on the Dynamics of Marine Vehicles and Structures in Waves, ed. Bishop, R.E.D. and Price, W.G., Mech. Eng. Pub. Ltd., London, 1975, pp. 258-277.

8. Jen, Y. — *Wave Forces on Circular Cylindrical Piles Used in Coastal Structures.* Univ. Calif., Berkeley, Rep. No. HEL 9-11, January 1967, 98 pp.

9. Kokkinowrachos, K. Wilckens, H. — *Hydrodynamic Analysis of Cylindrical Offshore Oil Storage Tanks.* Proc. Sixth Offshore Tech. Conf., Houston, Paper No. OTC 1944, 1974, pp. 99-112.

10. Lebreton, J.C. Cormault, P. — *Wave Action on Slightly Immersed Structures. Some Theoretical and Experimental Considerations.* Proc. Symp. Research on Wave Action, Delft Hydraulics Lab., Vol. IV, Paper 12A, 1969, 34 pp.

11. MacCamy, R.C.
Fuchs, R.A.
Wave Forces on Piles: A Diffraction Theory.
U.S. Army Beach Erosion Board, Tech. Memo. No. 69, December 1954, 17 pp.

12. Mogridge, G.R.
Jamieson, W.W.
A Design Method for the Estimation of Wave Loads on Square Caissons.
National Research Council Canada, DME, Hydraulics Lab. Tech. Rep. No. LTR-HY-57, 1976, 66 pp.

13. Morison, J.R.
O'Brien, M.P.
Johnson, J.W.
Schaaf, S.A.
The Force Exerted by Surface Waves on Piles.
J. Petrol. Technol., Vol. 189, 1950, pp. 149-154.

14. Pratte, B.D.
Funke, E.R.
Mogridge, G.R.
Jamieson, W.W.
Wave Forces on a Model Pile.
Proc. First Canadian Hydraulics Conf., Edmonton, 1973, pp. 523-543.

15. Raman, H.
Venkatanarasaiah, P.
Forces Due to Nonlinear Waves on Vertical Cylinders.
Proc. ASCE, Vol. 102, No. WW3, August 1976, pp. 301-316.

16. Van Oortmerssen, G.
Some Aspects of Very Large Offshore Structures.
Ninth Symp. Naval Hydrodynamics, Paris, Paper No. 17, August 1972.

17. Watanabe, A.
Horikawa, K.
Breaking Wave Forces on a Large Diameter Cell.
Proc. Fourteenth Coastal Eng. Conf., Copenhagen, 1974, pp. 1741-1760.

18. Yamaguchi, M.
Tsuchiya, Y.
Nonlinear Effect of Waves on Wave Pressure and Wave Force on a Large Cylindrical Pile.
(In Japanese), Proc. Civil Engineering Society in Japan, No. 229, September 1974, pp. 41-53.

19. Zwarts, C.M.G.
Noncontacting Capacitive Wave Transducers Part I.
NRC, DME Mechanical Engineering Report MI-836, National Research Council Canada, Ottawa, Ontario, 1972, 77 pp.

20. Zwarts, C.M.G.
Noncontacting Capacitive Wave Transducers Part II.
NRC, DME Mechanical Engineering Report MI-837, National Research Council Canada, Ottawa, Ontario, 1975, 48 pp.

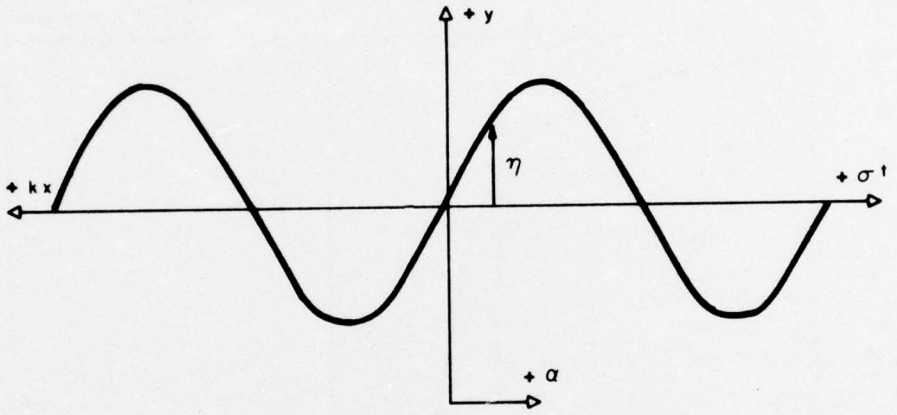

$$\eta = -\frac{H}{2} \sin (kx - \sigma t)$$

FIG. 1: CO-ORDINATE SYSTEM

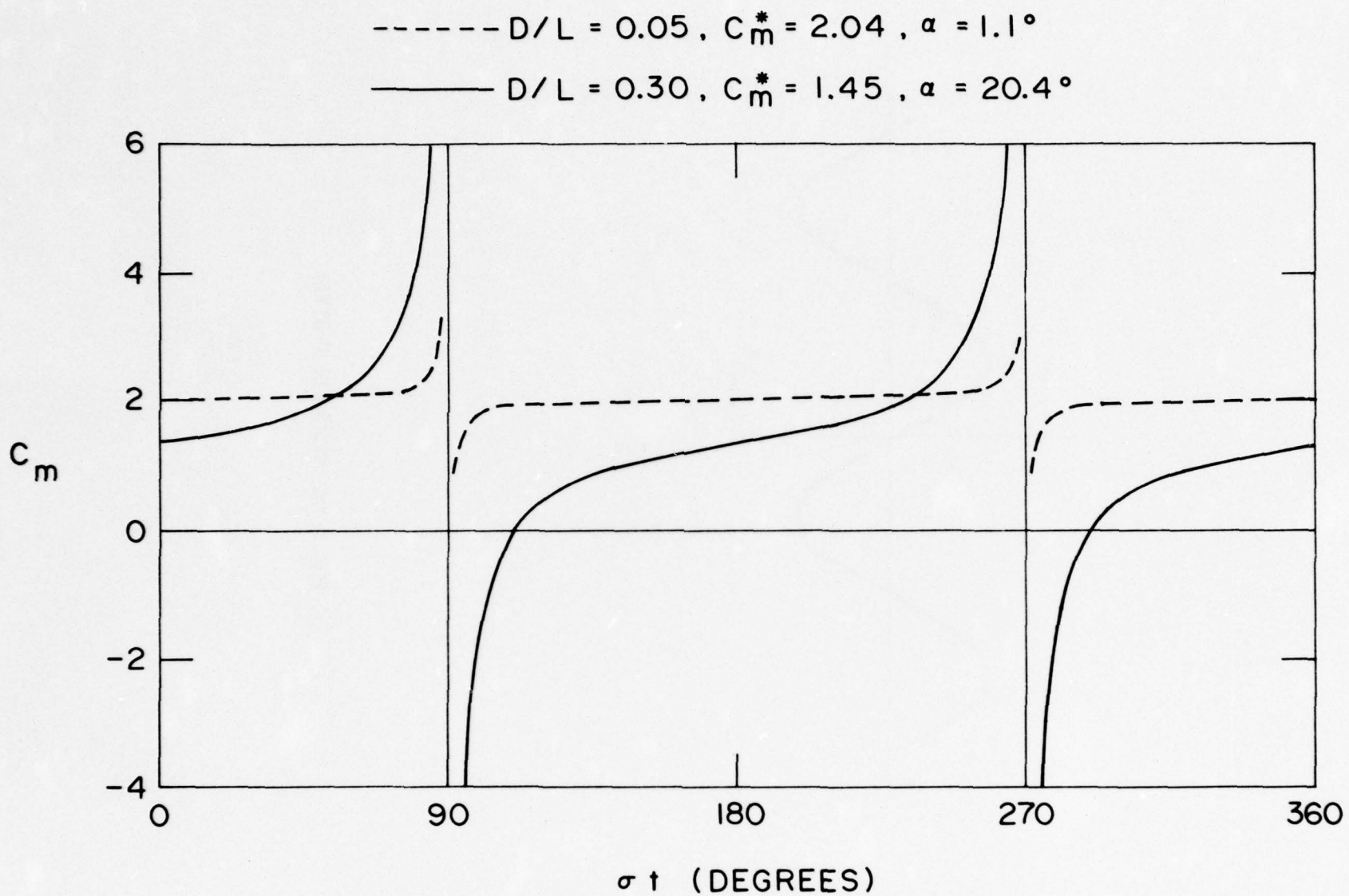

FIG. 2: VARIATION OF C_m THROUGH A WAVE CYCLE

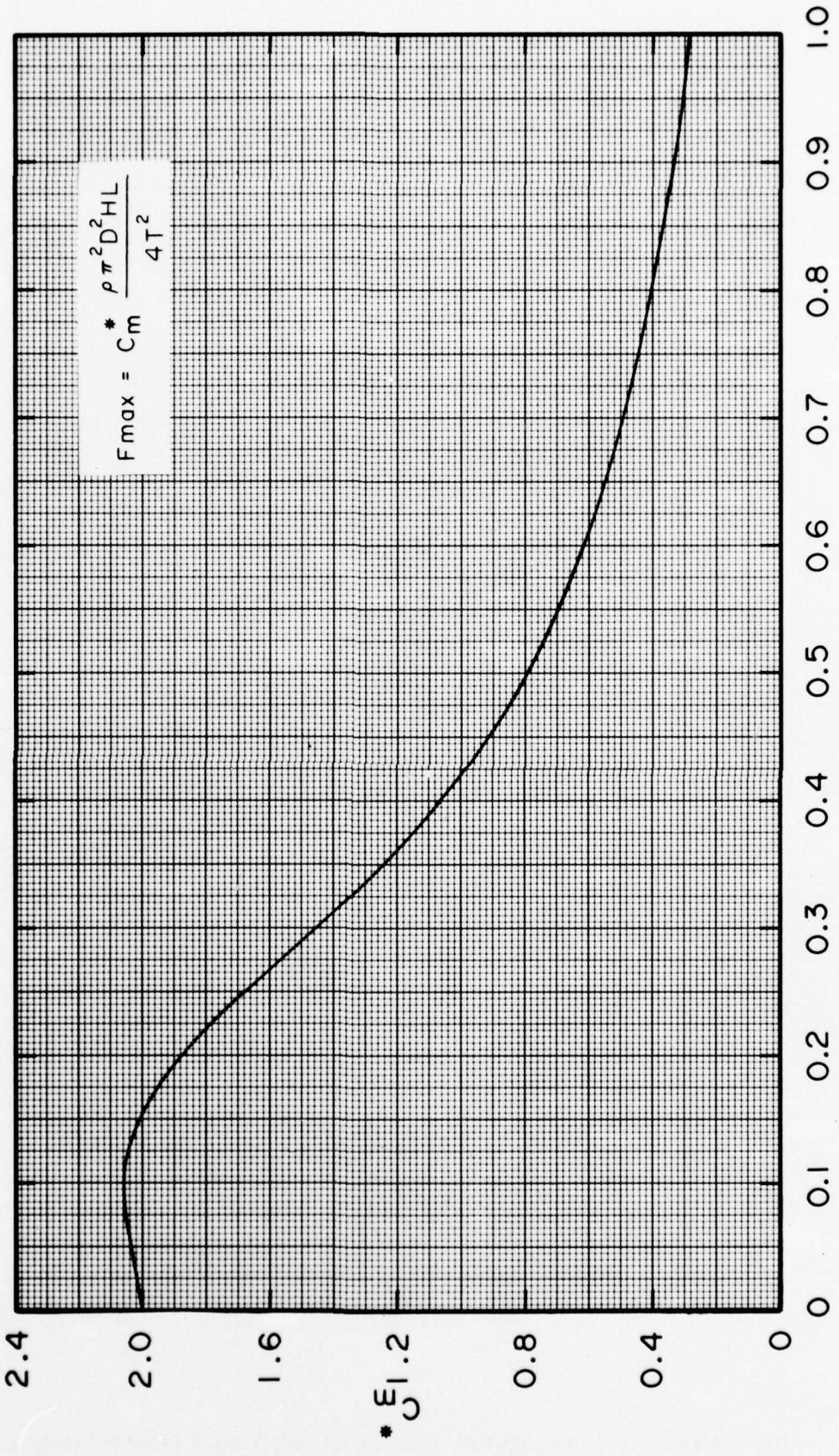

FIG. 3: C_m^* AS A FUNCTION OF D/L

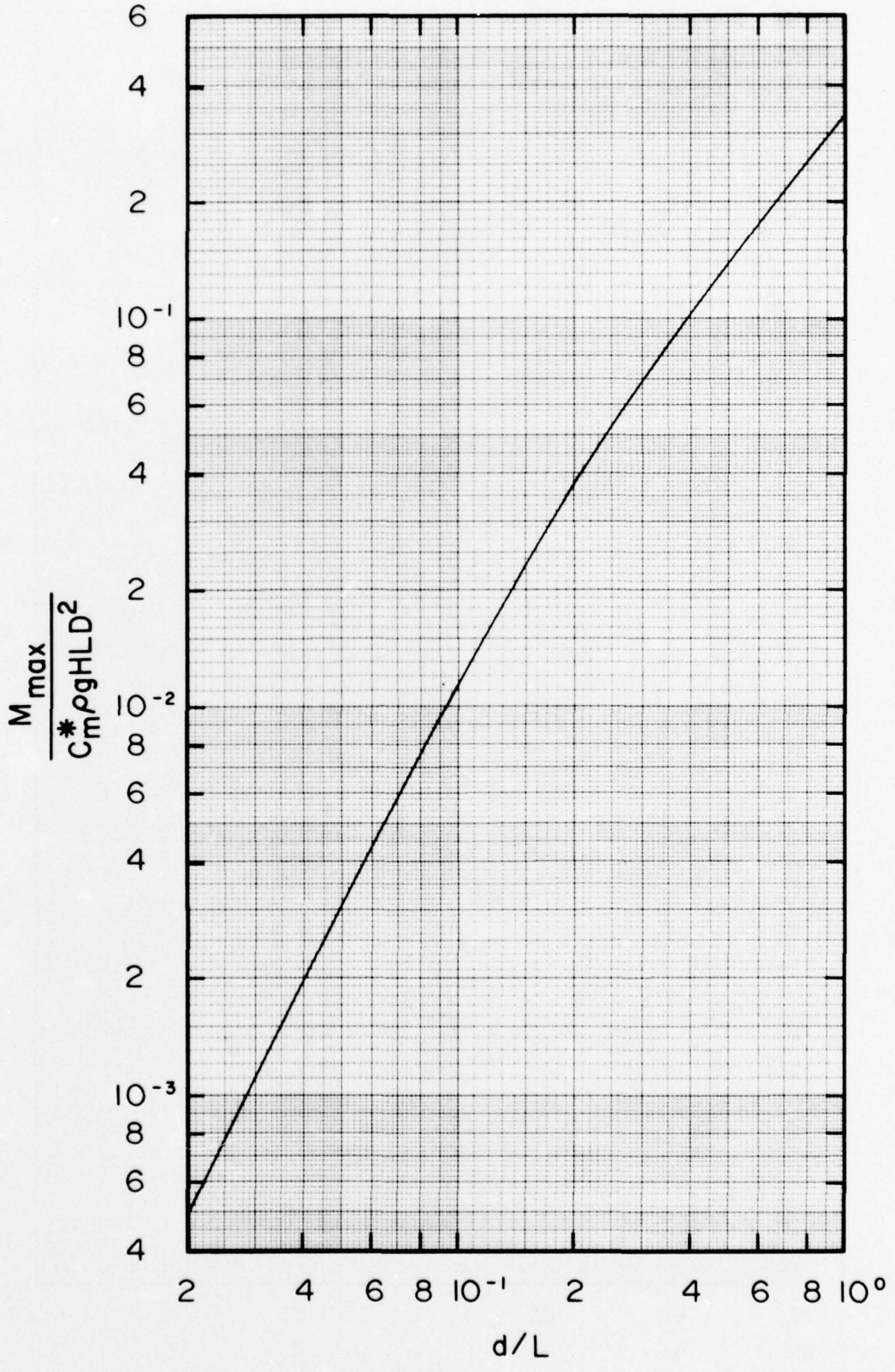

FIG. 4: DIMENSIONLESS OVERTURNING MOMENT AS A FUNCTION OF d/L

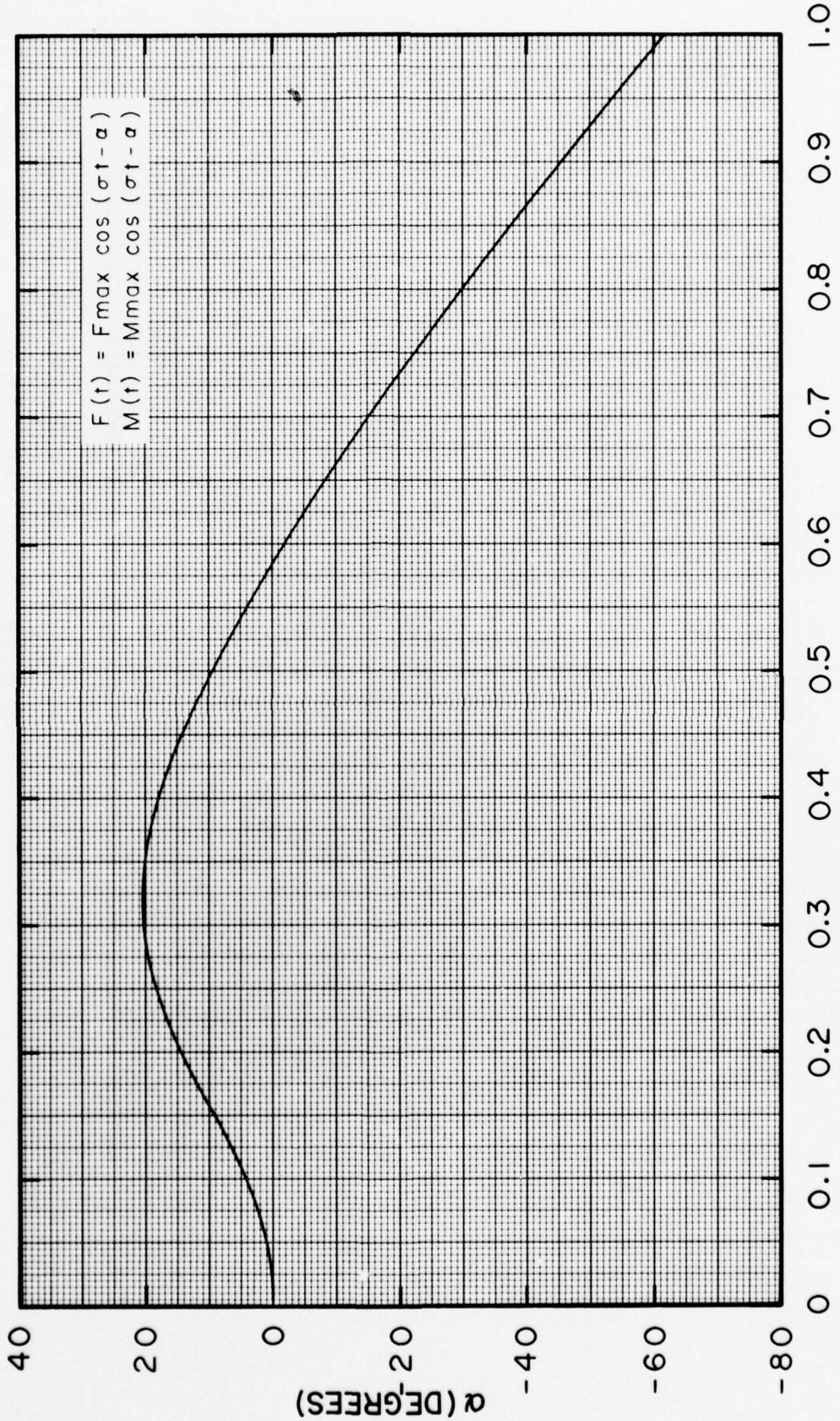

FIG. 5: PHASE ANGLE AS A FUNCTION OF D/L

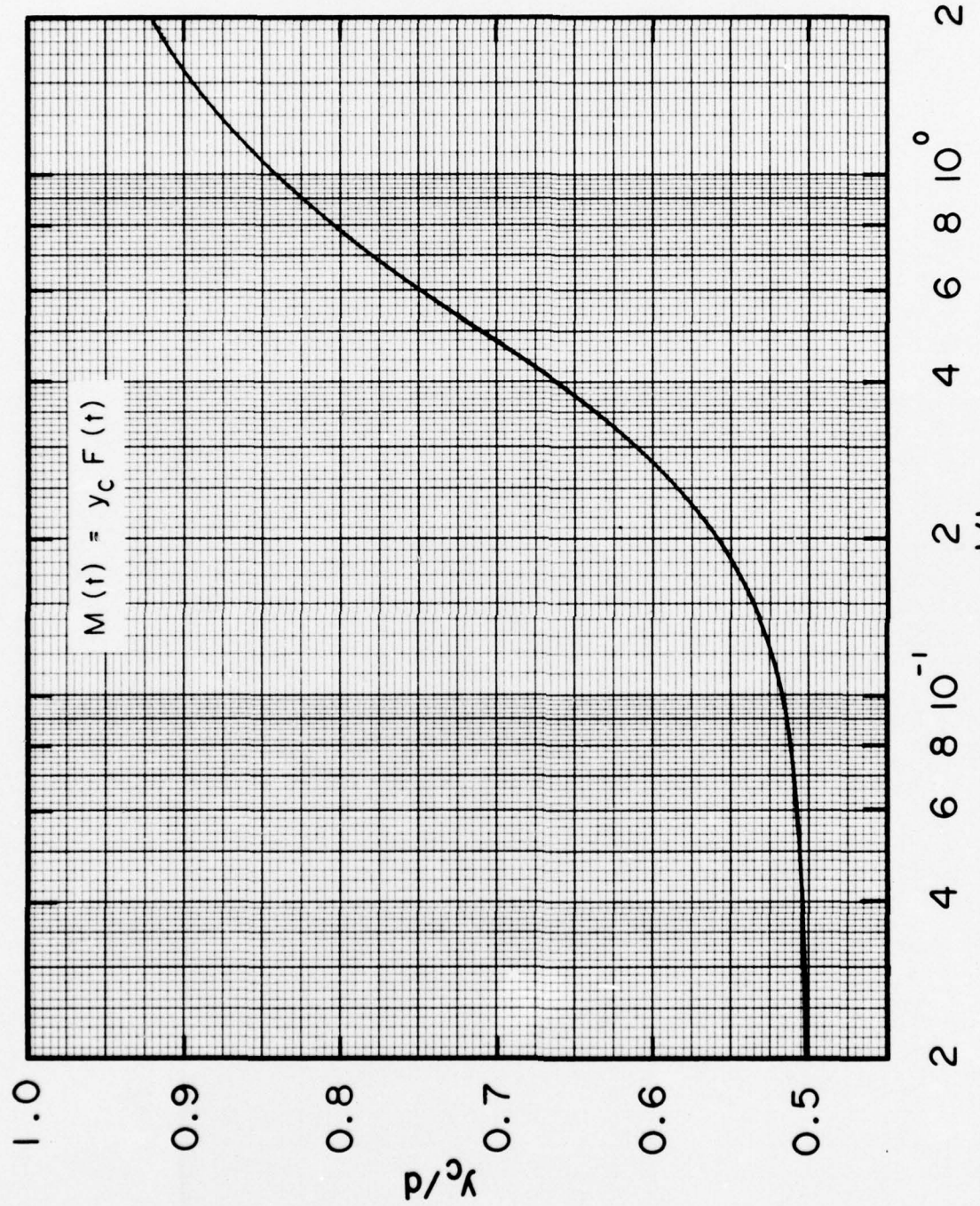

FIG. 6: DIMENSIONLESS LEVER ARM AS A FUNCTION OF d/L

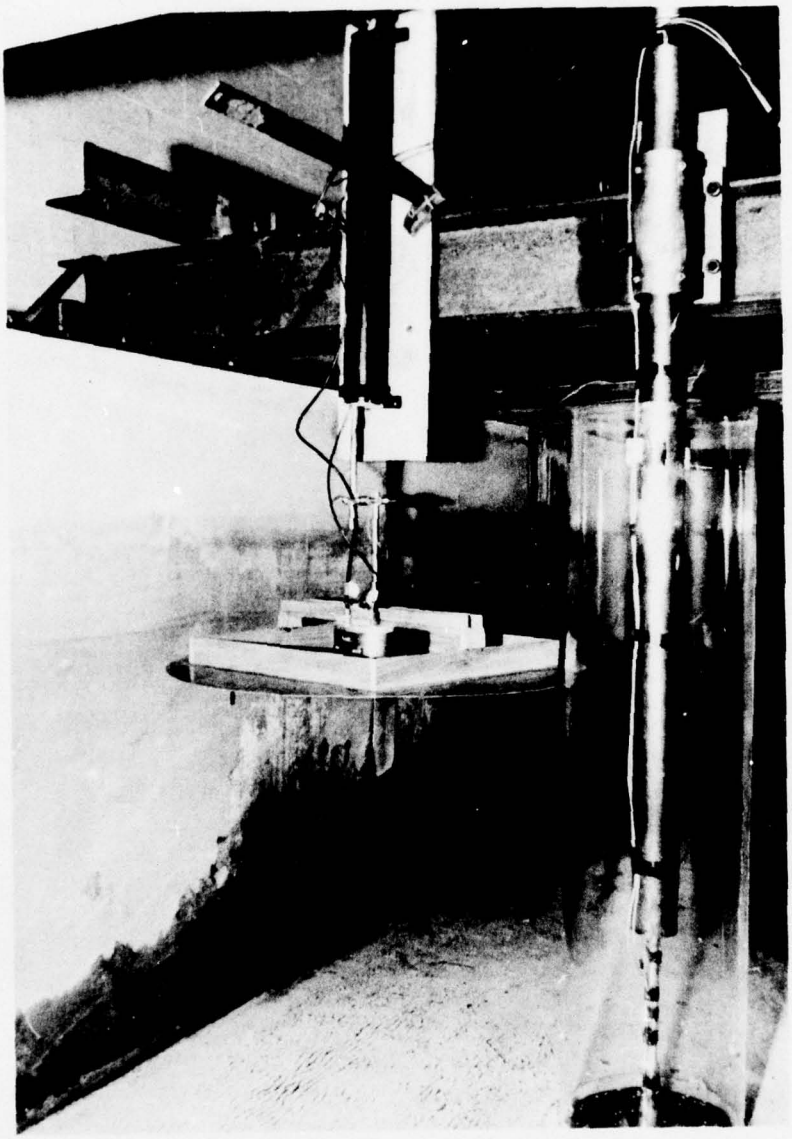

FIG. 7: CIRCULAR CYLINDER AND WAVE GAUGE

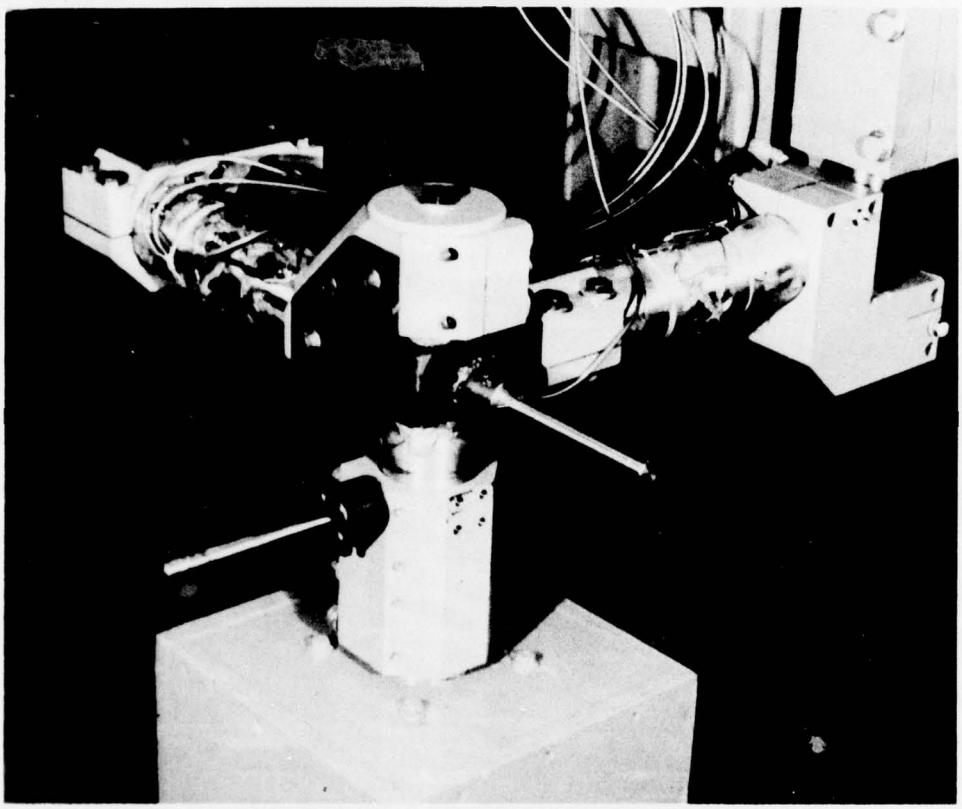

FIG. 8: SIX-COMPONENT FORCE METER

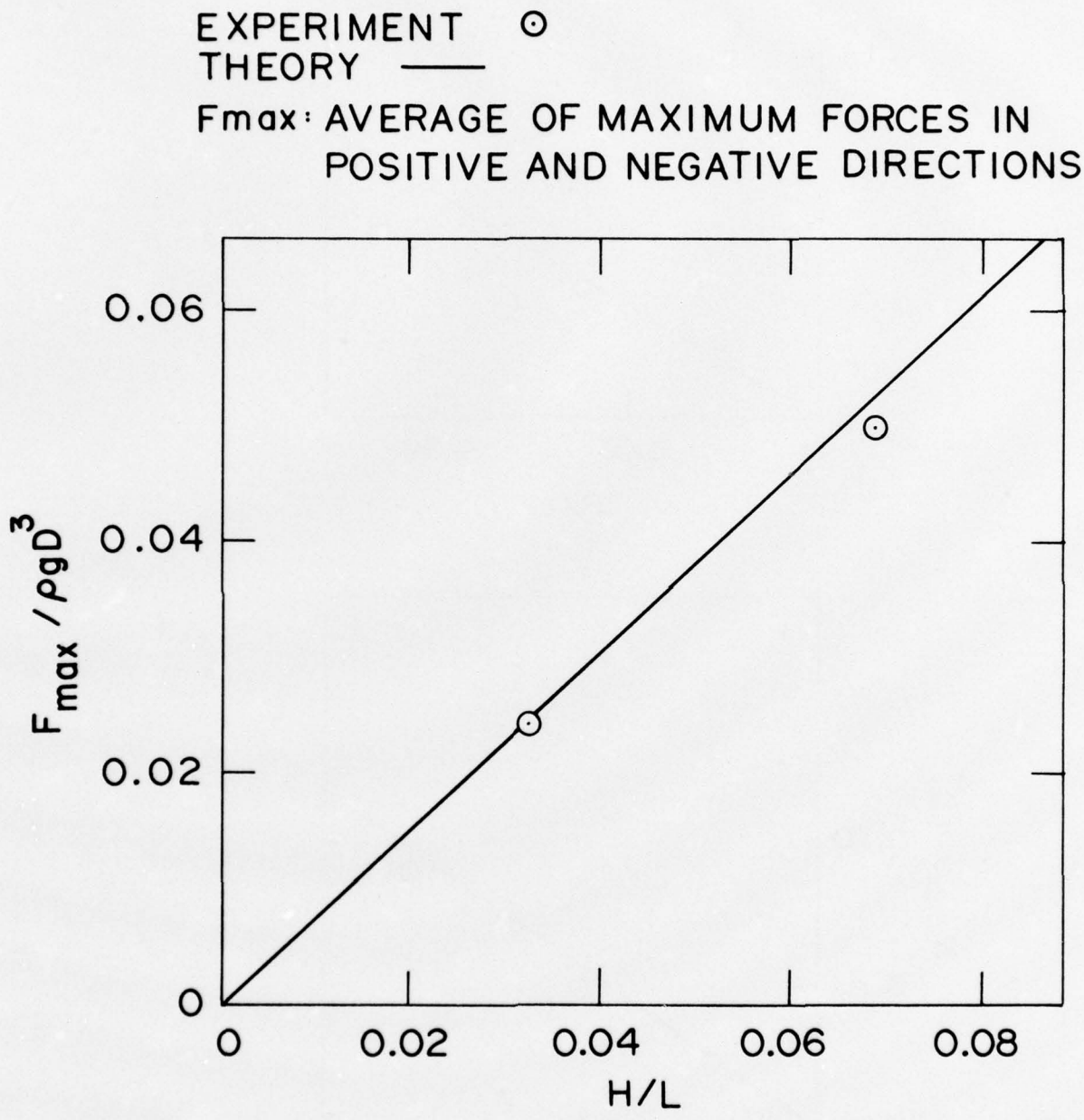

FIG. 9: MAXIMUM FORCES
(D/L = 0.441, d/L = 0.250)

EXPERIMENT ⊙
THEORY ——

Fmax, Mmax: AVERAGE OF MAXIMUM FORCES AND MOMENTS IN POSITIVE AND NEGATIVE DIRECTIONS

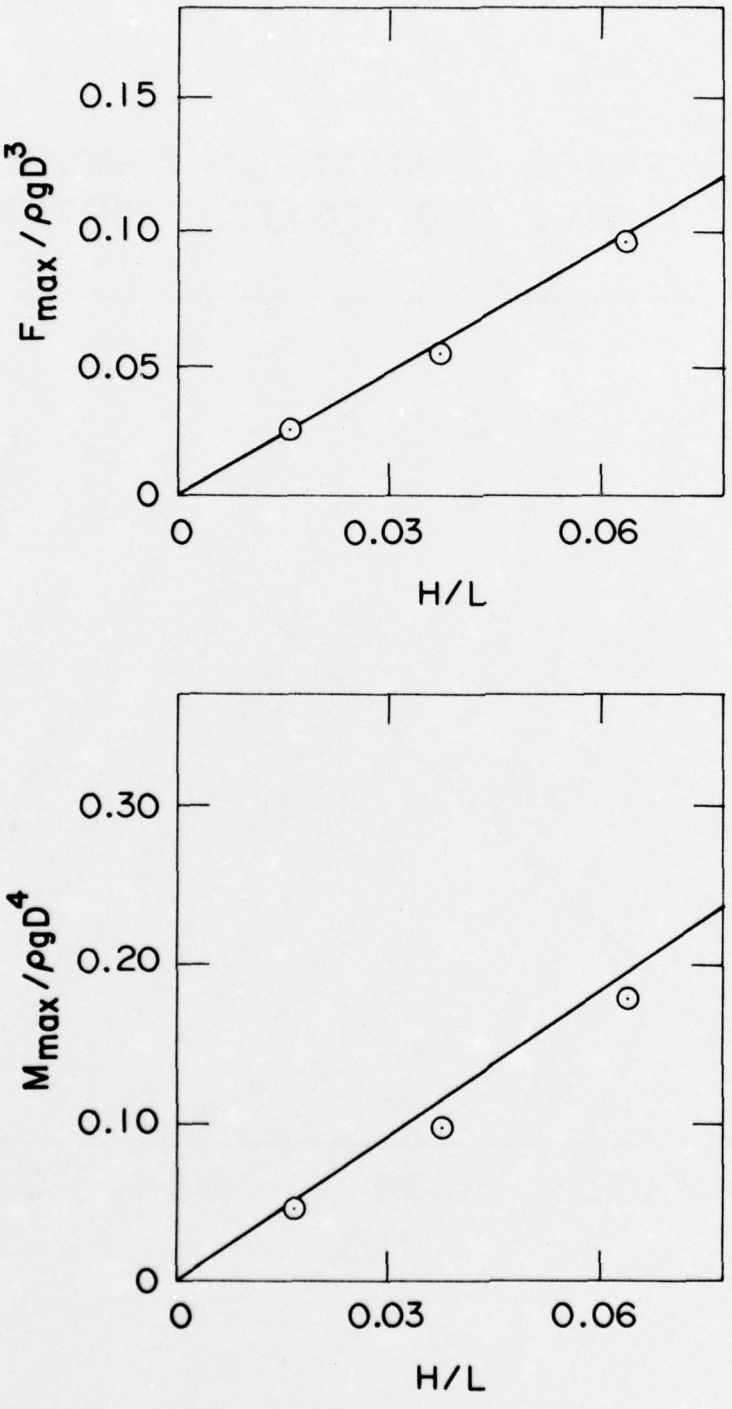

FIG. 10: MAXIMUM FORCES AND MOMENTS (D/L = 0.325, d/L = 0.786)

EXPERIMENT ⊙
THEORY ——
Fmax, Mmax : AVERAGE OF MAXIMUM FORCES AND MOMENTS IN POSITIVE AND NEGATIVE DIRECTIONS

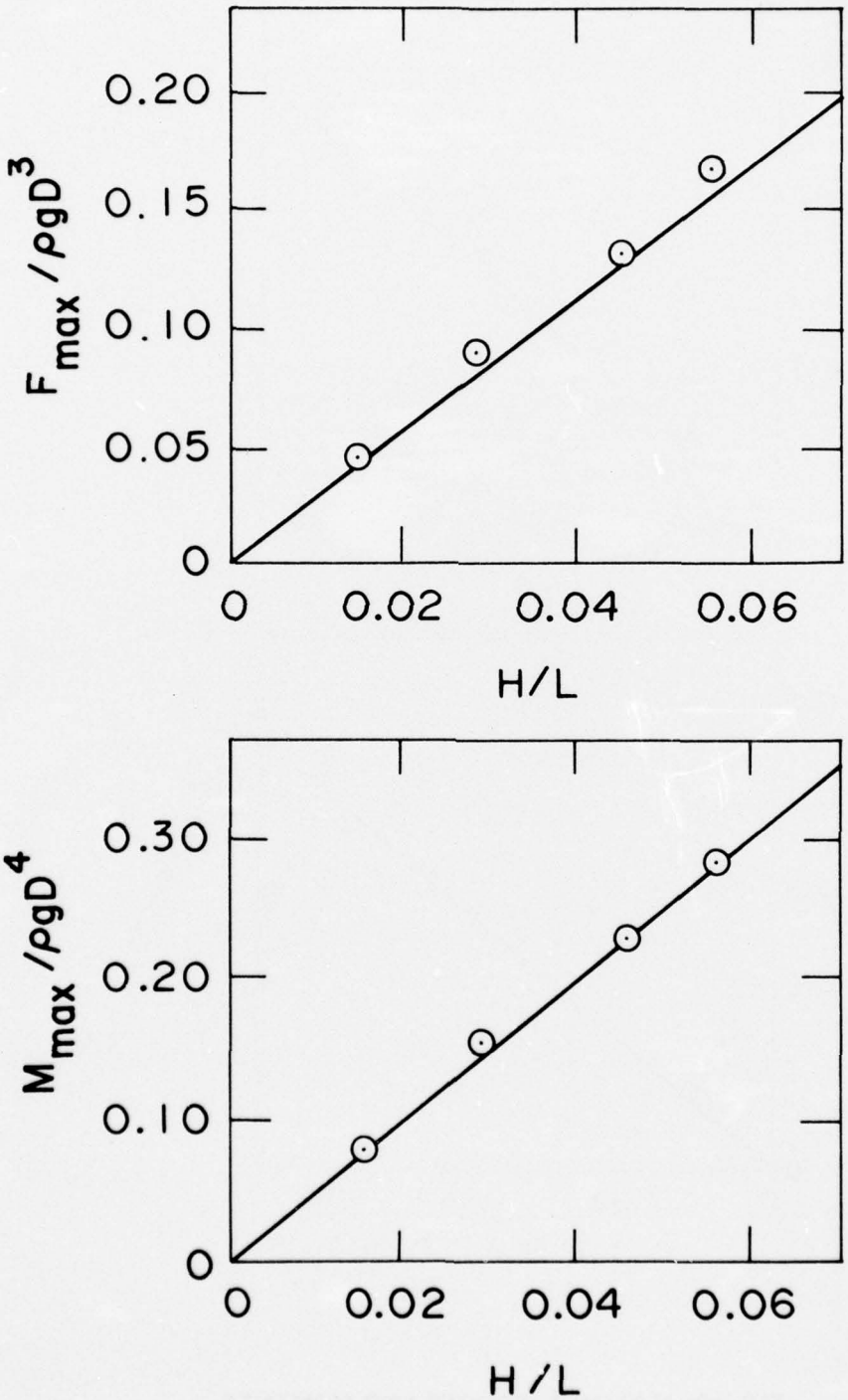

FIG. 11: MAXIMUM FORCES AND MOMENTS (D/L = 0.239, d/L = 0.578)

EXPERIMENT ⊙
THEORY ——
Fmax, Mmax: AVERAGE OF MAXIMUM FORCES AND MOMENTS IN POSITIVE AND NEGATIVE DIRECTIONS

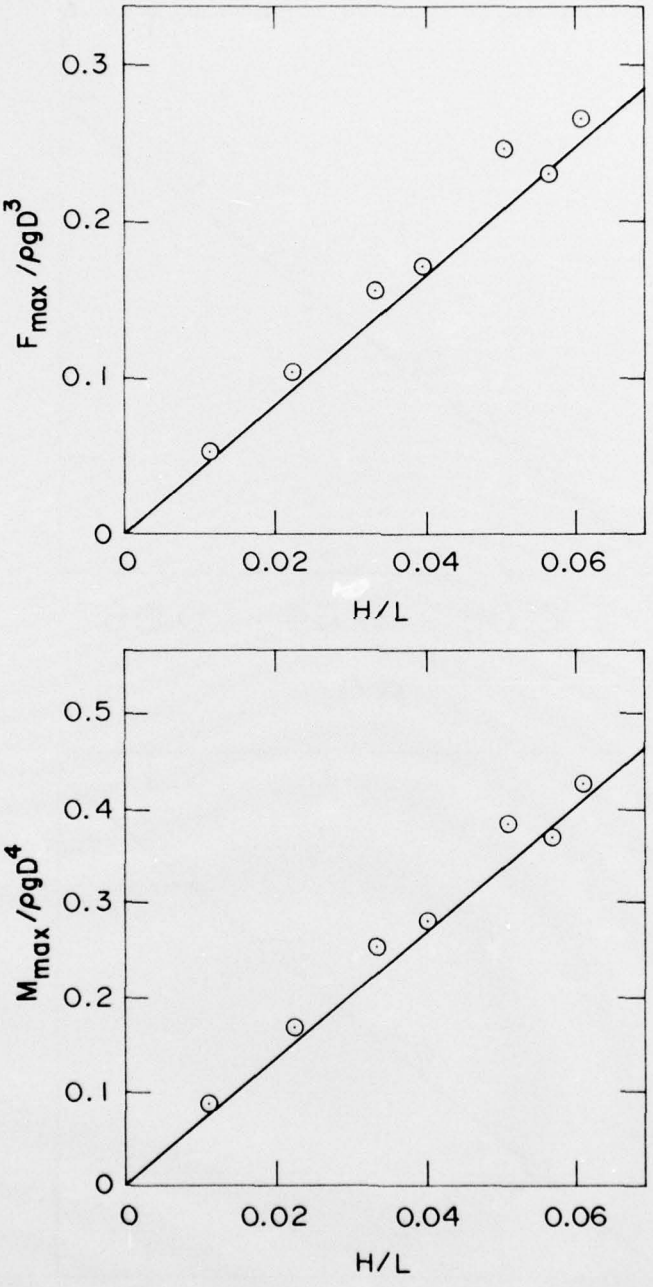

FIG. 12: MAXIMUM FORCES AND MOMENTS (D/L = 0.184, d/L = 0.445)

EXPERIMENT ⊙

THEORY ——

Fmax, Mmax: AVERAGE OF MAXIMUM FORCES AND MOMENTS IN POSITIVE AND NEGATIVE DIRECTIONS

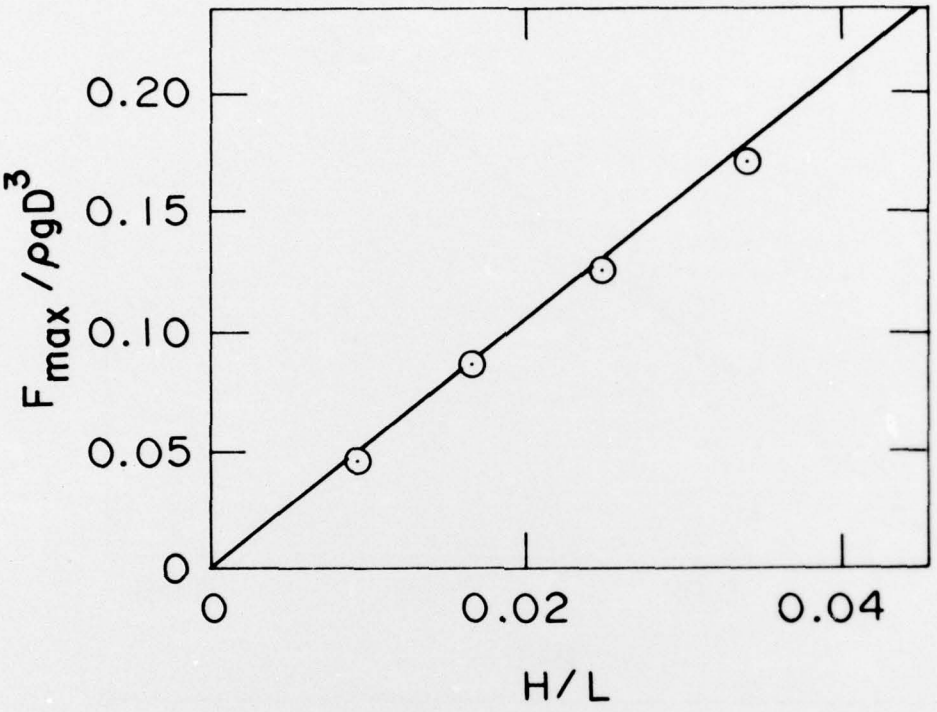

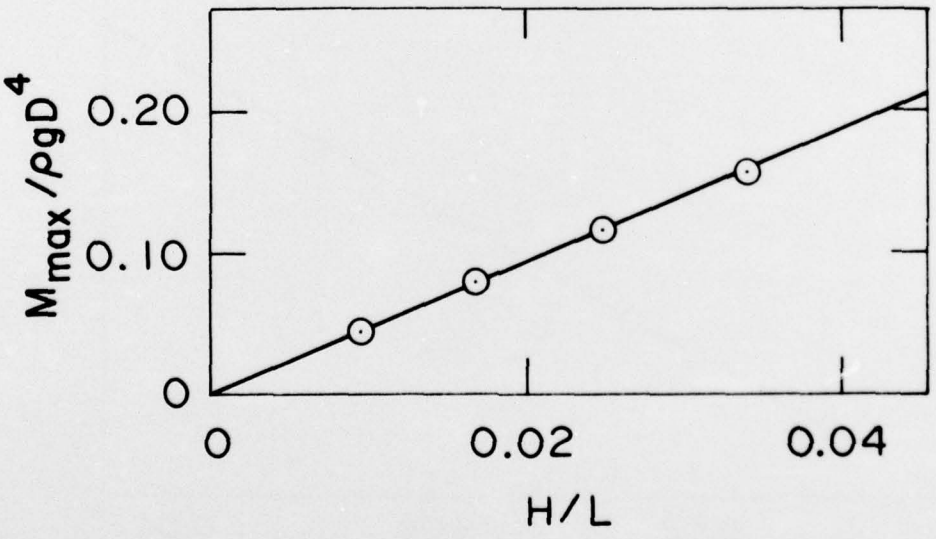

FIG. 13: MAXIMUM FORCES AND MOMENTS (D/L = 0.134, d/L = 0.213)

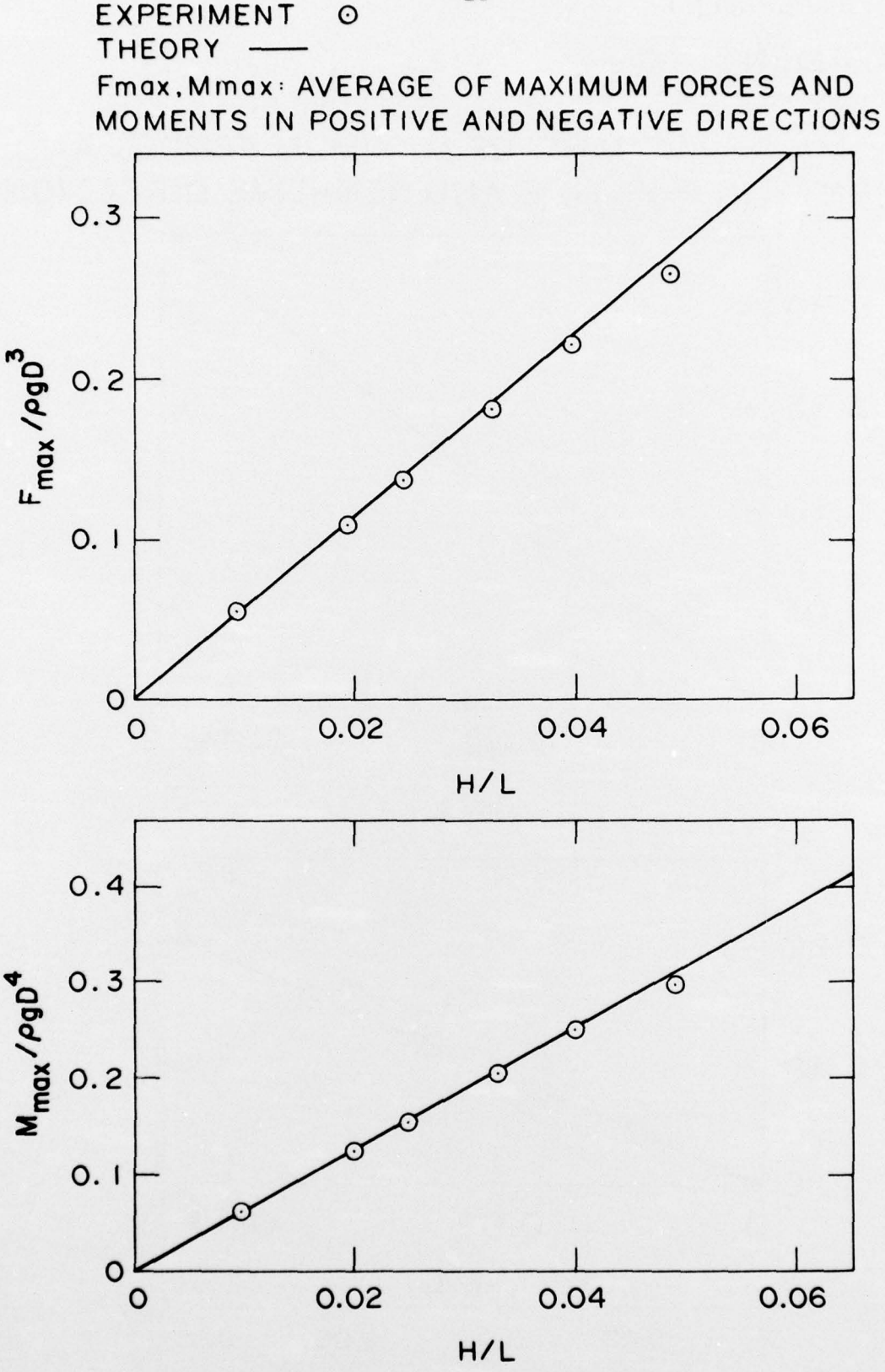

FIG. 14: MAXIMUM FORCES AND MOMENTS (D/L = 0.128, d/L = 0.246)

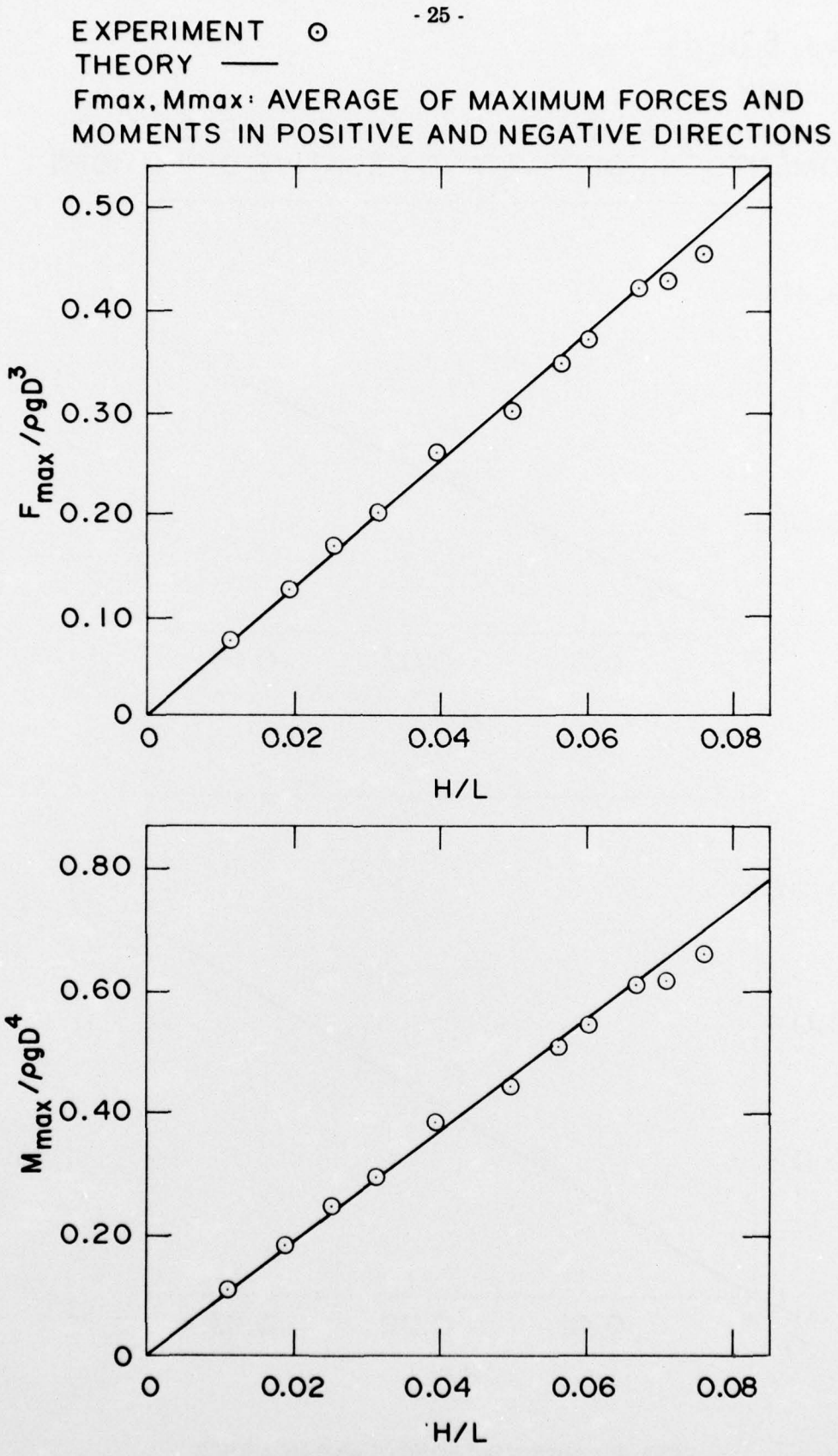

FIG. 15: MAXIMUM FORCES AND MOMENTS (D/L = 0.123, d/L = 0.297)

EXPERIMENT ⊙
THEORY ——
Fmax, Mmax: AVERAGE OF MAXIMUM FORCES AND MOMENTS IN POSITIVE AND NEGATIVE DIRECTIONS

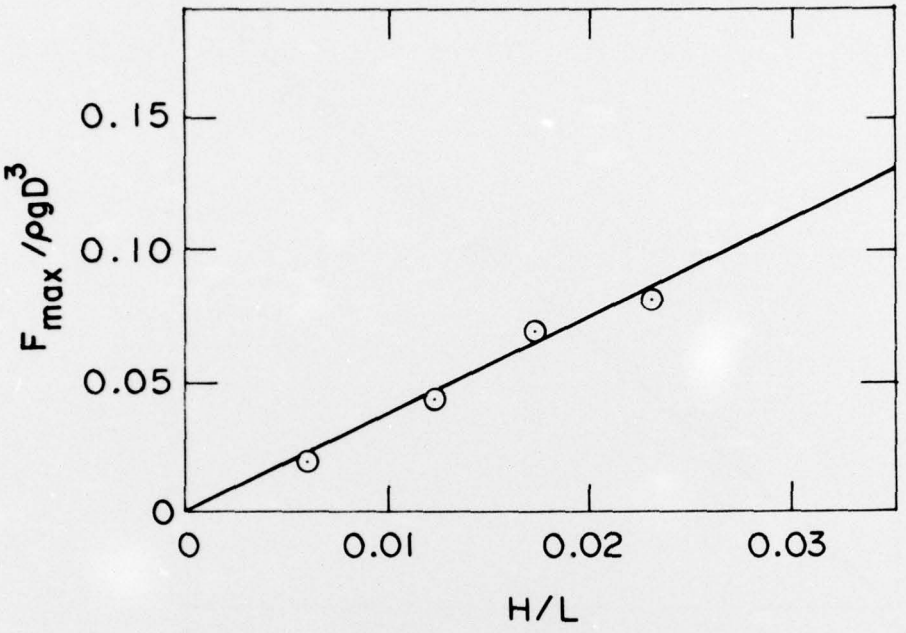

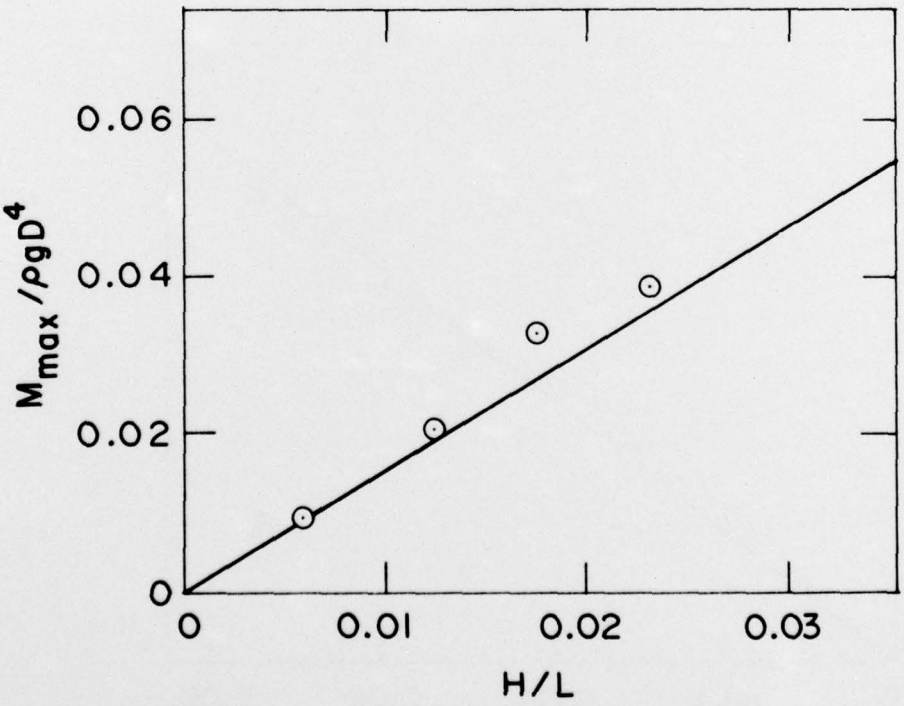

FIG. 16: MAXIMUM FORCES AND MOMENTS (D/L = 0.114, d/L = 0.092)

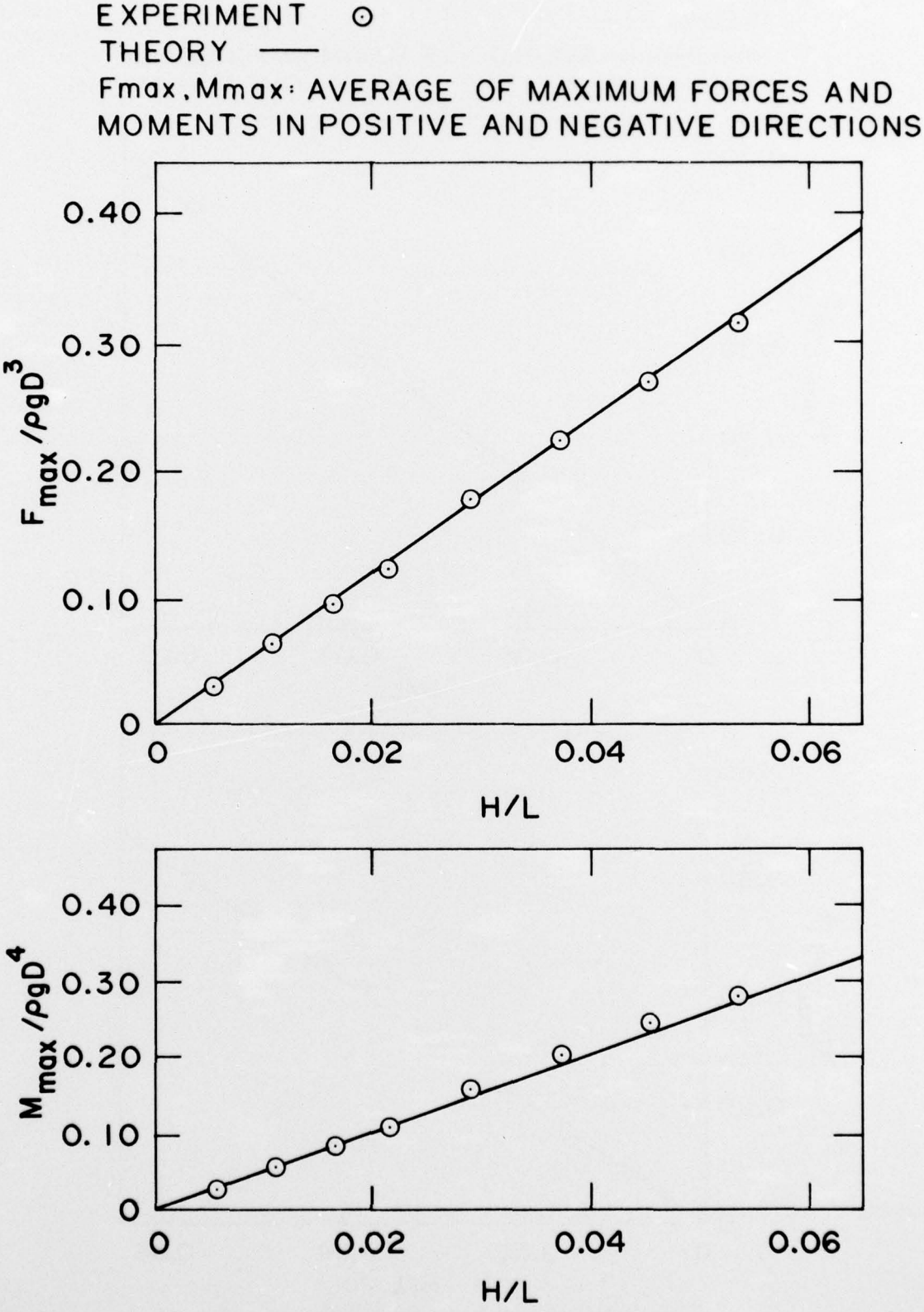

FIG. 17: MAXIMUM FORCES AND MOMENTS (D/L = 0.105, d/L = 0.165)

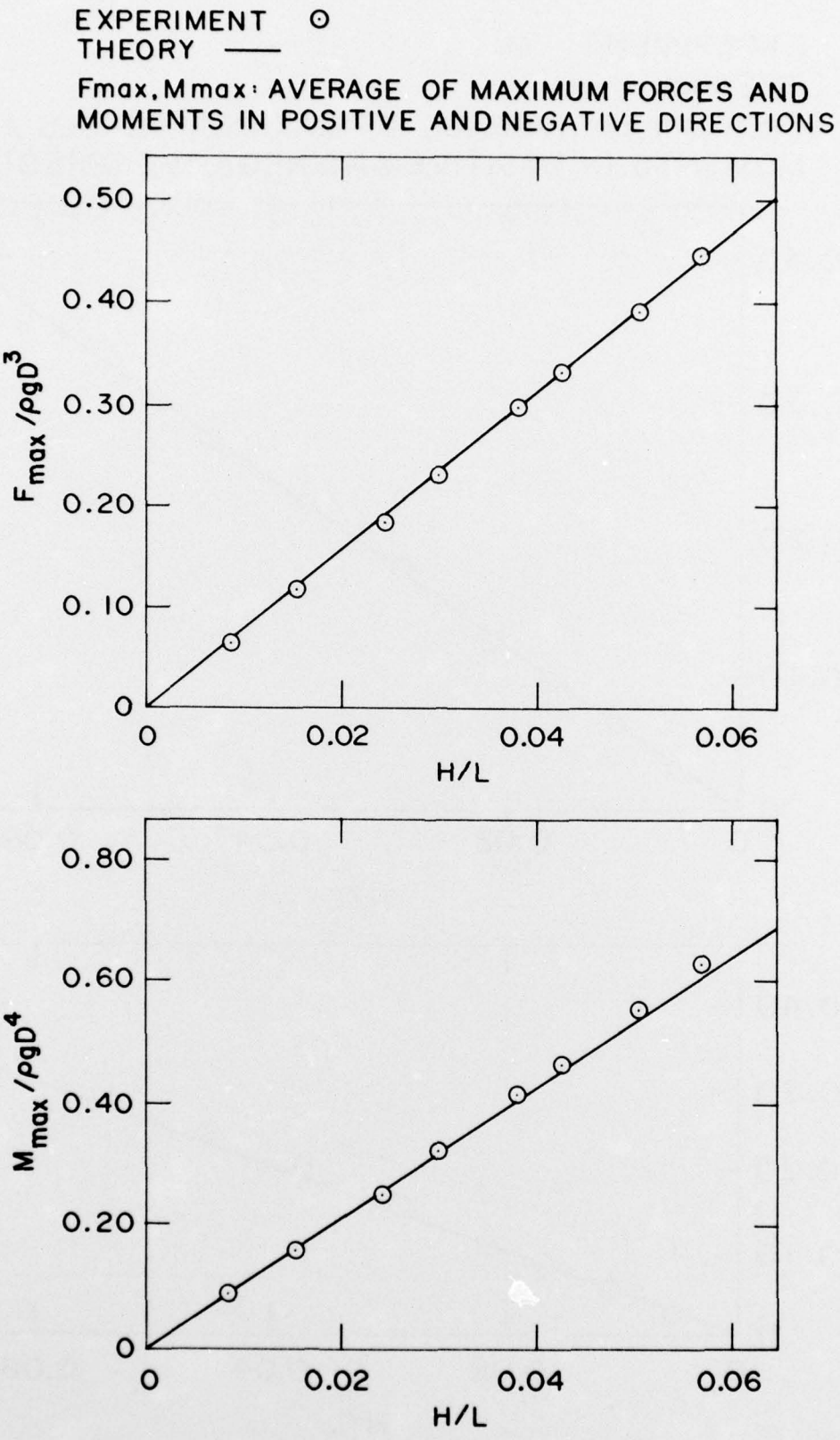

FIG. 18: MAXIMUM FORCES AND MOMENTS (D/L = 0.092, d/L = 0.222)

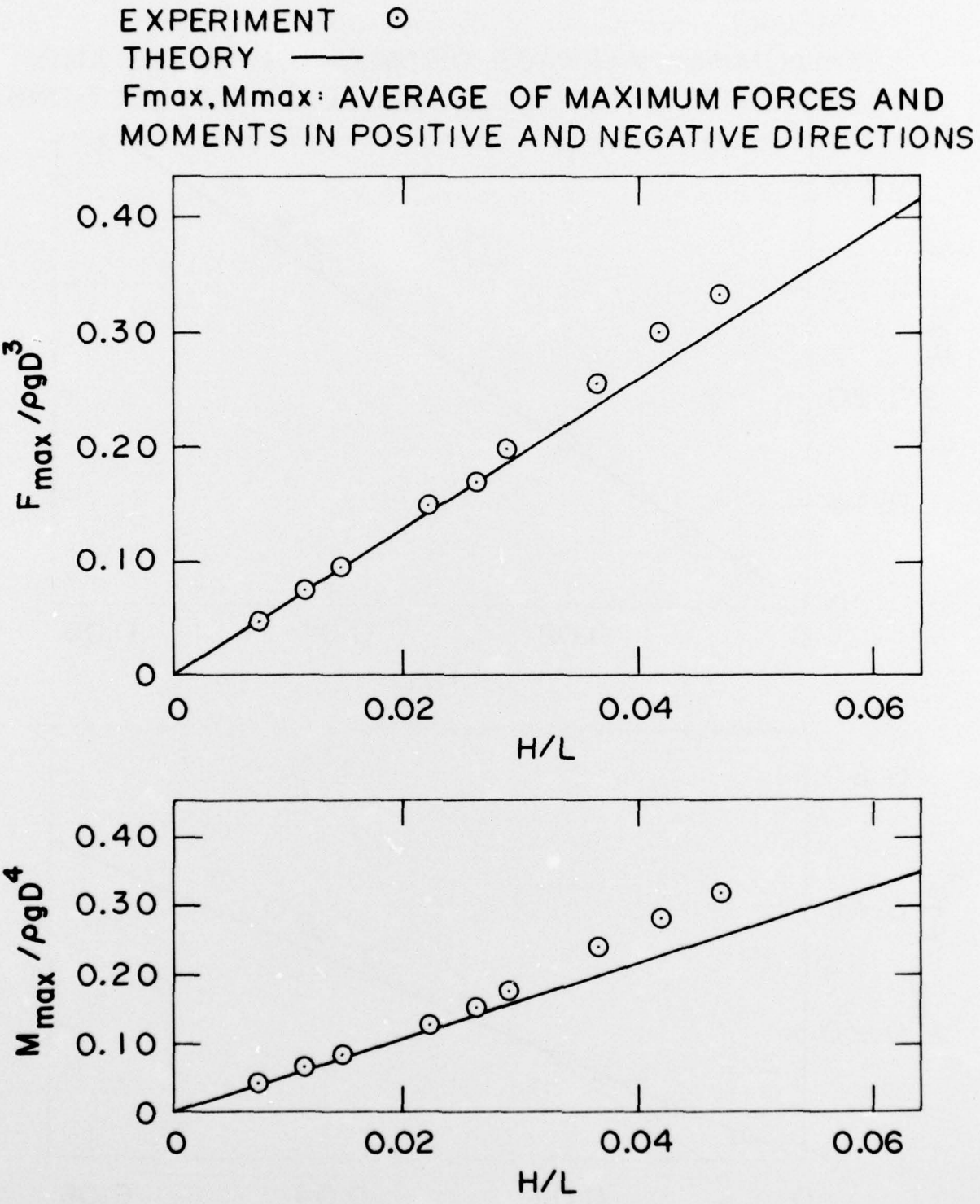

FIG. 19: MAXIMUM FORCES AND MOMENTS
(D/L = 0.086, d/L = 0.136)

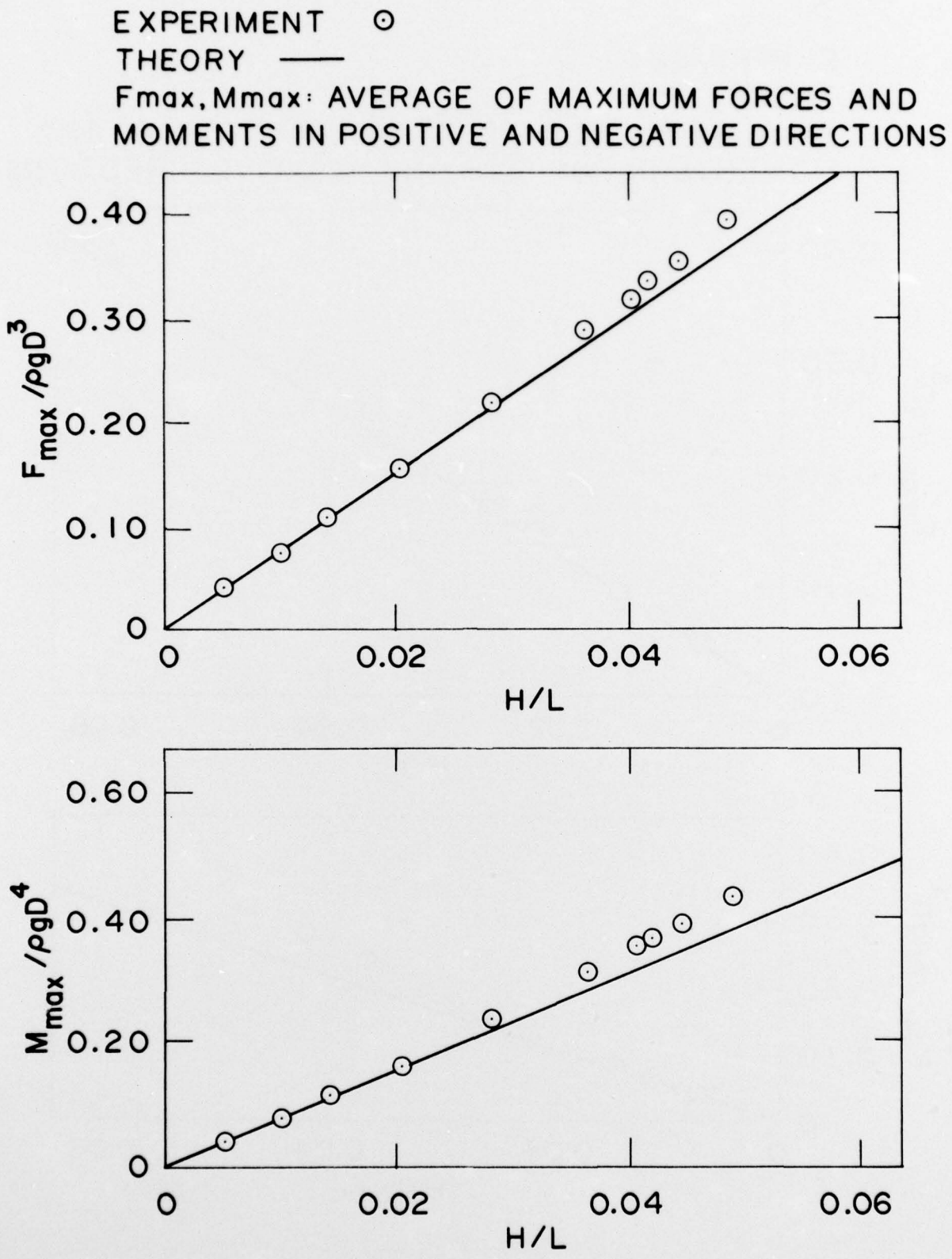

FIG. 20: MAXIMUM FORCES AND MOMENTS (D/L = 0.080, d/L = 0.153)

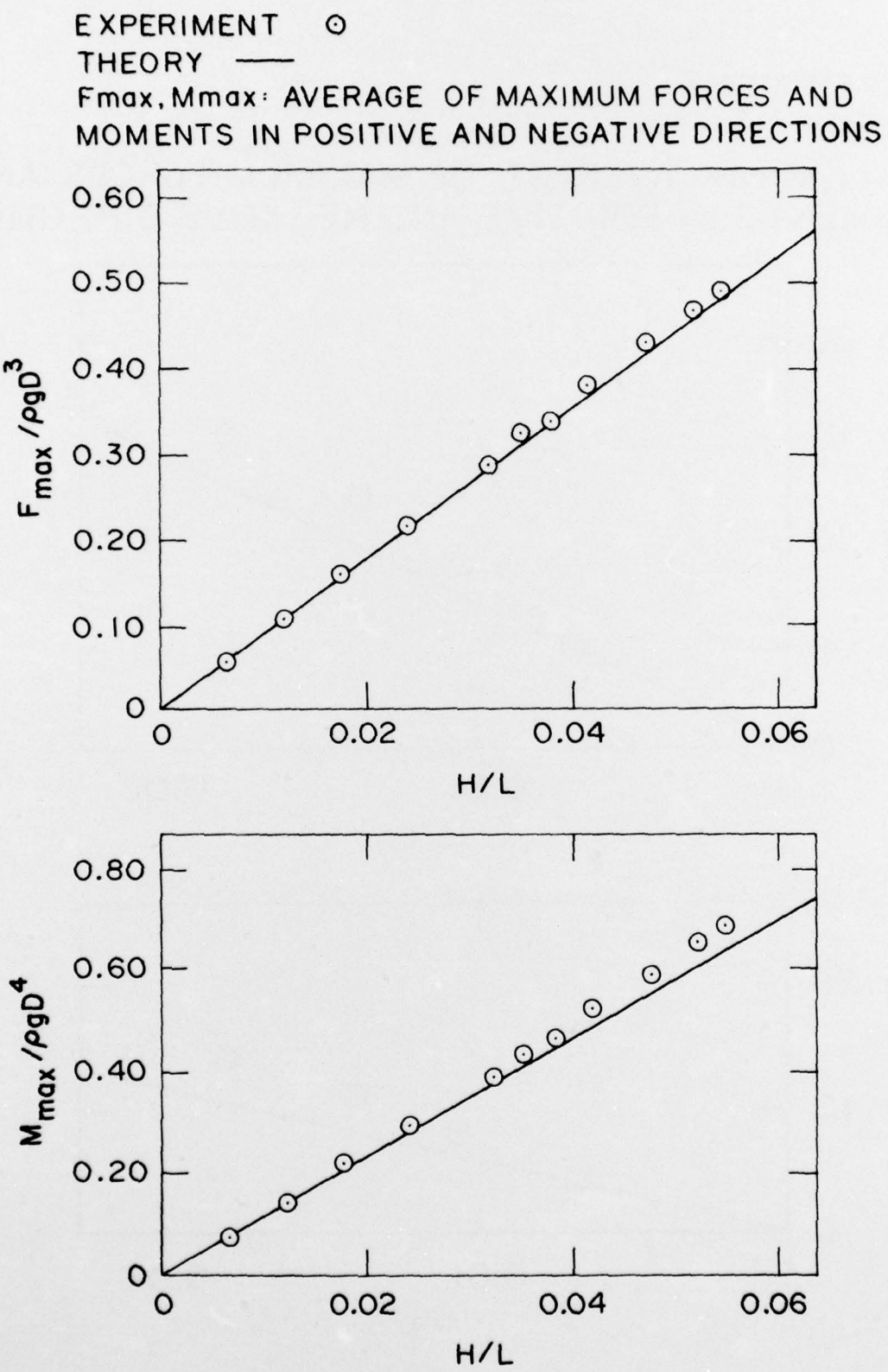

FIG. 21: MAXIMUM FORCES AND MOMENTS
(D/L = 0.074, d/L = 0.179)

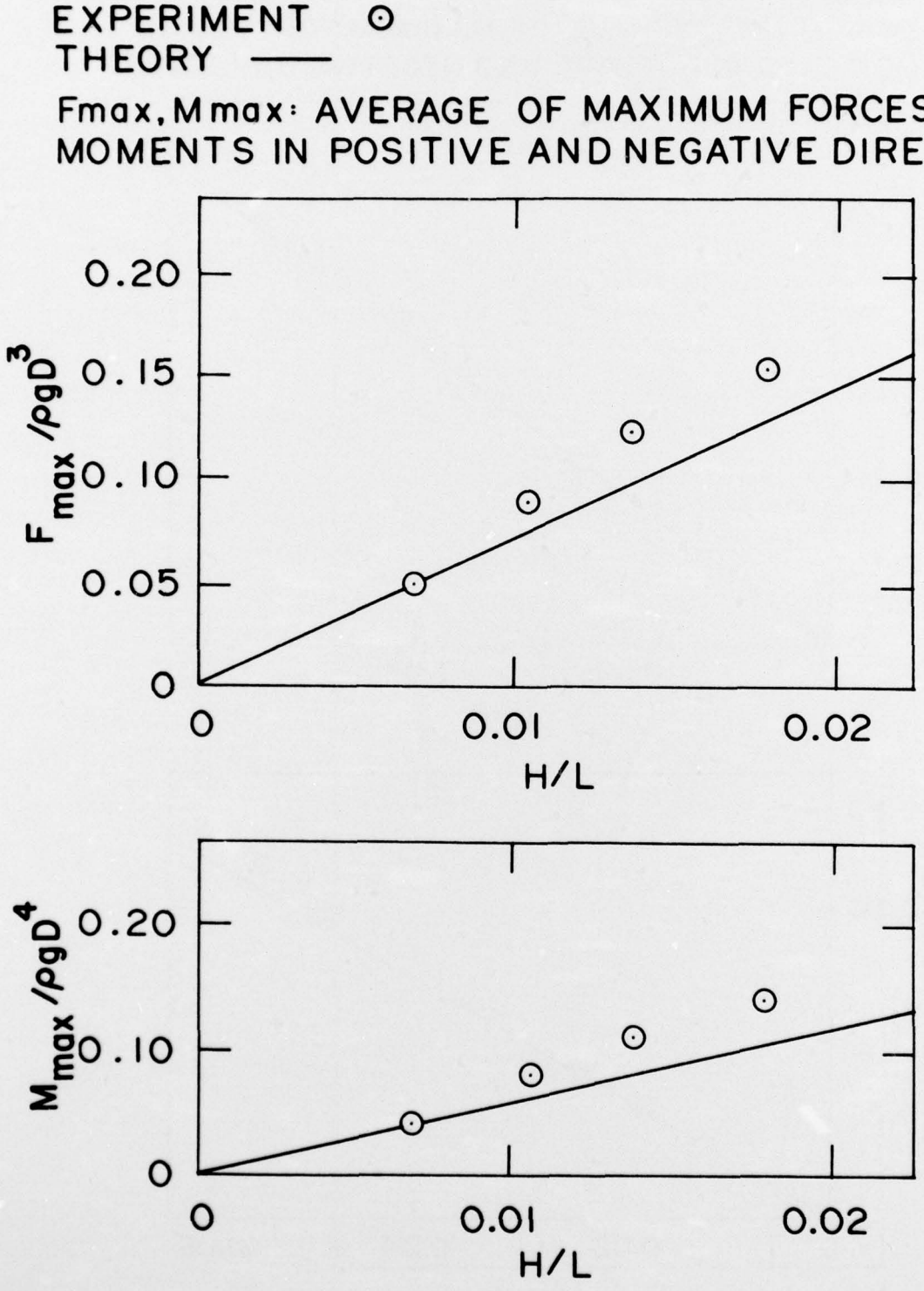

FIG. 22: MAXIMUM FORCES AND MOMENTS (D/L = 0.057, d/L = 0.090)

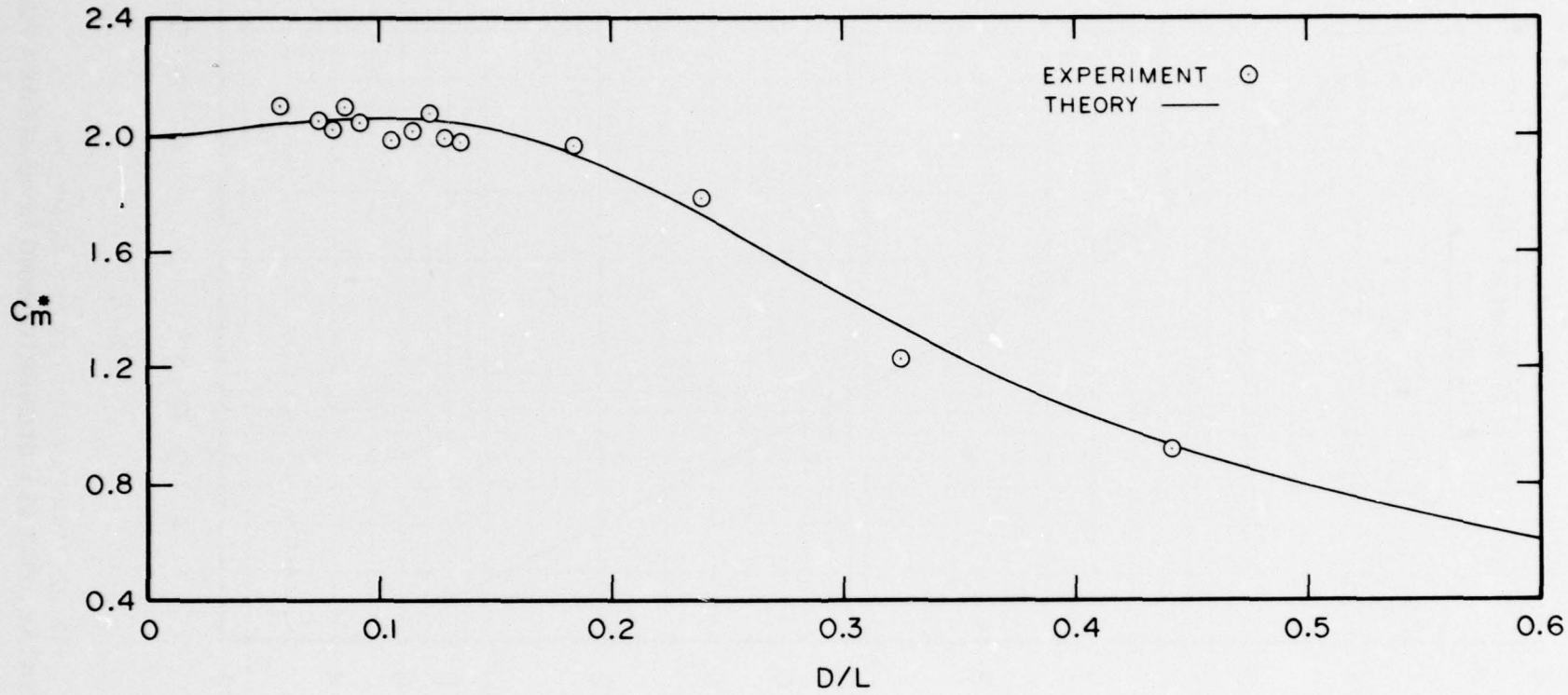

FIG. 23: EXPERIMENTAL RESULTS FOR C_m^* AS A FUNCTION OF D/L

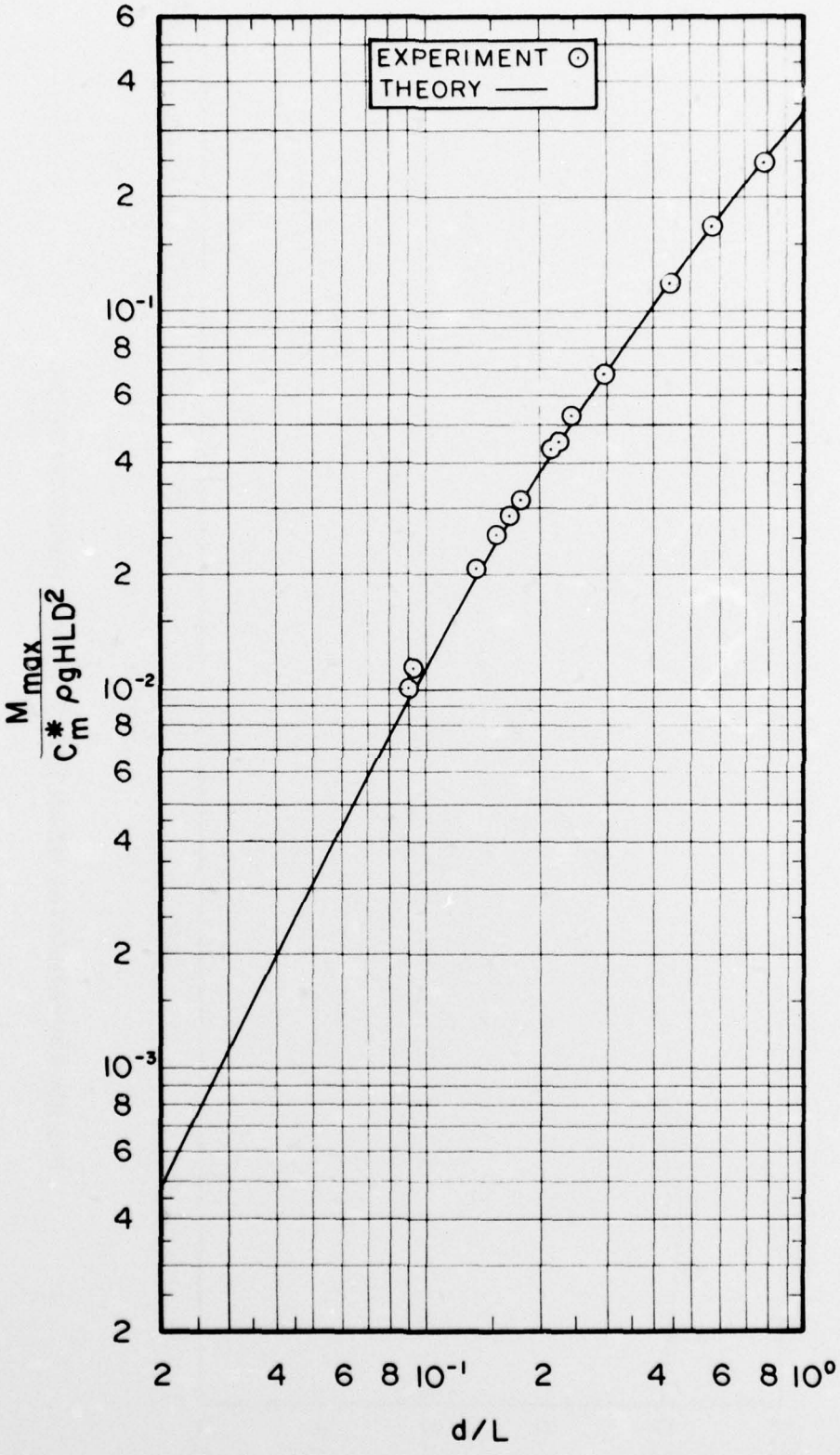

FIG. 24: EXPERIMENTAL RESULTS FOR OVERTURNING MOMENTS AS A FUNCTION OF d/L

Page 35

NRC, DME MH-111
National Research Council Canada. Division of Mechanical Engineering.

WAVE LOADS ON LARGE CIRCULAR CYLINDERS: A DESIGN METHOD.
Mogridge, G.R., Jamieson, W.W. December 1976. 40 pp. (incl. figures).

The forces and overturning moments exerted by waves on large vertical circular cylinders have been measured in the laboratory. Two rigid cylinders, 12 in. and 26.5 in. in diameter, extending from the bottom of a wave flume through the water surface, were tested in varying depths of water, for a range of wave periods and wave heights up to the point of breaking. A digital computer was used for the acquisition, processing, plotting and storage of the experimental data.

In addition to the experimental work, a design method is presented which allows the wave loads on large circular cylinders to be estimated by means of a simple desk calculation. The experimental data shows that this simple method of calculation, based on the linear diffraction theory of MacCamy and Fuchs, is accurate over a wide range of wave conditions and cylinder sizes.

UNCLASSIFIED

1. Cylinders — Water impingement.
2. Water waves.

I. Mogridge, G.R.
II. Jamieson, W.W.
III. NRC, DME MH-111

NRC, DME MH-111
National Research Council Canada. Division of Mechanical Engineering.

WAVE LOADS ON LARGE CIRCULAR CYLINDERS: A DESIGN METHOD.
Mogridge, G.R., Jamieson, W.W. December 1976. 40 pp. (incl. figures).

The forces and overturning moments exerted by waves on large vertical circular cylinders have been measured in the laboratory. Two rigid cylinders, 12 in. and 26.5 in. in diameter, extending from the bottom of a wave flume through the water surface, were tested in varying depths of water, for a range of wave periods and wave heights up to the point of breaking. A digital computer was used for the acquisition, processing, plotting and storage of the experimental data.

In addition to the experimental work, a design method is presented which allows the wave loads on large circular cylinders to be estimated by means of a simple desk calculation. The experimental data shows that this simple method of calculation, based on the linear diffraction theory of MacCamy and Fuchs, is accurate over a wide range of wave conditions and cylinder sizes.

UNCLASSIFIED

1. Cylinders — Water impingement.
2. Water waves.

I. Mogridge, G.R.
II. Jamieson, W.W.
III. NRC, DME MH-111

NRC, DME MH-111
National Research Council Canada. Division of Mechanical Engineering.

WAVE LOADS ON LARGE CIRCULAR CYLINDERS: A DESIGN METHOD.
Mogridge, G.R., Jamieson, W.W. December 1976. 40 pp. (incl. figures).

The forces and overturning moments exerted by waves on large vertical circular cylinders have been measured in the laboratory. Two rigid cylinders, 12 in. and 26.5 in. in diameter, extending from the bottom of a wave flume through the water surface, were tested in varying depths of water, for a range of wave periods and wave heights up to the point of breaking. A digital computer was used for the acquisition, processing, plotting and storage of the experimental data.

In addition to the experimental work, a design method is presented which allows the wave loads on large circular cylinders to be estimated by means of a simple desk calculation. The experimental data shows that this simple method of calculation, based on the linear diffraction theory of MacCamy and Fuchs, is accurate over a wide range of wave conditions and cylinder sizes.

UNCLASSIFIED

1. Cylinders — Water impingement.
2. Water waves.

I. Mogridge, G.R.
II. Jamieson, W.W.
III. NRC, DME MH-111

NRC, DME MH-111
National Research Council Canada. Division of Mechanical Engineering.

WAVE LOADS ON LARGE CIRCULAR CYLINDERS: A DESIGN METHOD.
Mogridge, G.R., Jamieson, W.W. December 1976. 40 pp. (incl. figures).

The forces and overturning moments exerted by waves on large vertical circular cylinders have been measured in the laboratory. Two rigid cylinders, 12 in. and 26.5 in. in diameter, extending from the bottom of a wave flume through the water surface, were tested in varying depths of water, for a range of wave periods and wave heights up to the point of breaking. A digital computer was used for the acquisition, processing, plotting and storage of the experimental data.

In addition to the experimental work, a design method is presented which allows the wave loads on large circular cylinders to be estimated by means of a simple desk calculation. The experimental data shows that this simple method of calculation, based on the linear diffraction theory of MacCamy and Fuchs, is accurate over a wide range of wave conditions and cylinder sizes.

UNCLASSIFIED

1. Cylinders — Water impingement.
2. Water waves.

I. Mogridge, G.R.
II. Jamieson, W.W.
III. NRC, DME MH-111